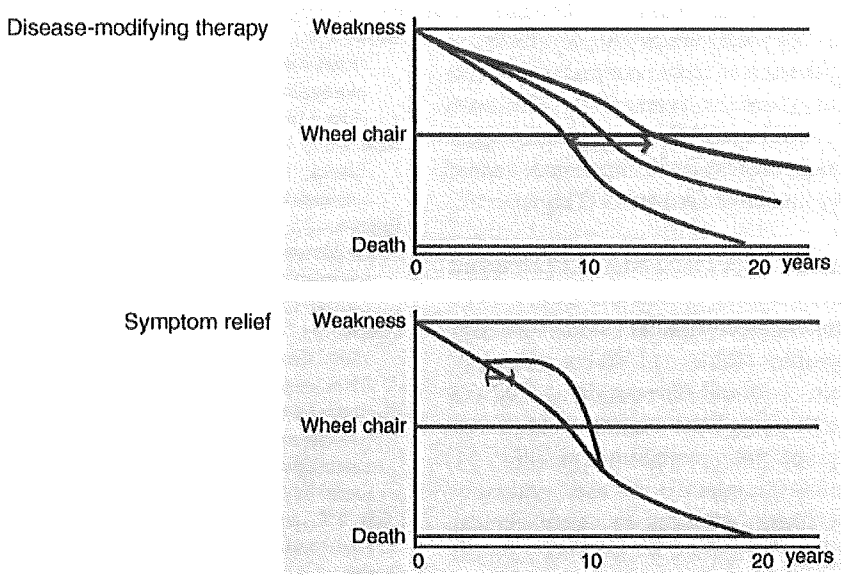


Fig. 5. Disease-modifying therapy and symptom relief. Since the goal of disease-modifying therapy is to inhibit pathogenic progression, long-term trials need to be carried out in order to evaluate drug effects by targeting certain clinical events as the primary endpoint. On the other hand, symptom relief, such as replacement of neurotransmitter, is used to ameliorate symptoms resulting from neurodegeneration. Although trial duration tends to be short, the effect of this therapy is often transient. Arrows indicate trial duration required for each therapy.

inhibitors have been considered to be of therapeutic benefit in polyglutamine diseases (Steffan et al., 2001, Hockly et al., 2003). Butyrate is the first HDAC inhibitor to be discovered, and the related compound, phenylbutyrate, has been successfully employed in experimental cancer therapy. Oral administration of sodium butyrate ameliorates symptomatic and histopathological phenotypes of our mouse model of SBMA through upregulation of histone acetylation in nervous tissues (Minamiyama et al., 2004). Although sodium butyrate is likely to be a promising treatment of SBMA, this compound yielded beneficial effects only within a narrow therapeutic window of dosage in the mouse model. Careful dose determination is mandatory when using HDAC inhibitors for treatment of polyglutamine diseases.

### *Axonal trafficking defects in SBMA*

Motor neurons possess extremely long axon along which molecular motors transport essential components such as organelles, vesicles, cytoskeletons, and signal molecules. This implies that axonal trafficking plays a fundamental role in maintenance of normal function of motor neurons. Obstruction of axonal transport has gained attention as a cause of neuronal dysfunction in a variety of neurodegenerative diseases including SBMA (Gunawardena and Goldstein, 2005). A mutation in the gene of proteins regulating axonal trafficking, dynein and dynactin 1, has been shown to cause motor neuron degeneration in both human and rodent (Puls et al., 2003; Hafezparast et al., 2003). Experimental data suggest that axonal transport might be retarded by pathogenic polyglutamine-containing AR (Szebenyi et al., 2003). Although this notion is intriguing, its contribution to the pathogenesis of SBMA should be further investigated, since aggregation of the pathogenic AR is rarely found within the axon of motor neurons in patients or model mice.

## Clinical application of potential therapeutics

Analysis of cellular and animal models provides insight into mechanisms involved in neurodegeneration of SBMA and indicates retinal therapeutic approaches to this disease (Fig. 4). Therapeutic agent candidates for SBMA are grossly classified into two groups: (i) drugs inhibiting accumulation of the pathogenic AR protein and (ii) drugs mitigating downstream pathological events including

Table1
Summary of therapeutic trials in SBMA mouse models

| Treatment | Number of mice (per treatment group) | Increase in survival (%) | Rotarod task | Body weight | AR accumulation | Reference |
|---|---|---|---|---|---|---|
| Castration | 6 | >120% | Improved | Improved | Decreased | Katsuno et al. (2002) |
| Castration[a] | 8–9 | Not determined | Improved | No effect | Decreased | Chevalier-Larsen et al. (2004) |
| Leuprorelin | 6 | >130% | Improved | Improved | Decreased | Katsuno et al. (2003) |
| Flutamide | 6 | No effect | No effect | No effect | No effect | Katsuno et al. (2003) |
| Sodium butyrate | 12–15 | 56% | Improved | Improved | No effect | Minamiyama et al. (2004) |
| 17-AAG | 27 | >60% | Improved | Improved | Decreased | Waza et al. (2005) |
| GGA | 12–15 | >60% | Improved | Improved | Decreased | Katsuno et al. (2005) |

[a] Treatment is initiated after the onset of motor impairment. AR, androgen receptor; 17-AAG, 17-allylamino geldanamycin; GGA, geranylgeranylacetone.

transcriptional dysregulation. The ideal therapy for polyglutamine diseases appears to be a combination of these potential therapeutic strategies, since each drug has potential adverse effects when used in a long term (Agrawal et al., 2005). In addition to pharmacological approaches, genetic interventions such as RNA interference can be applied if safety and delivery problems are solved (Caplen et al., 2002).

Since various therapeutic strategies for SBMA have emerged thanks to animal models recapitulating human diseases, it is of utmost importance to pursue intensive clinical studies to verify the results from animal studies (Table 1). When we apply candidate agents for patients, it should be considered that the majority of therapeutics emerging form animal studies are disease-modifying therapy, but not symptom-relief (Fig. 5). Given that SBMA is a slowly progressive disease, extremely long-term clinical trials are likely necessary to verify clinical benefits of disease-modifying therapies by targeting clinical endpoints such as occurrence of aspiration pneumonia or becoming wheelchair-bound. Suitable surrogate endpoints, which reflect the pathogenesis and severity of SBMA, are thus substantial to assess the therapeutic efficacy in drug trials. To this end, appropriate biomarkers should be identified and validated in translational researches.

## Acknowledgments

Fig. 2 is reproduced from Katsuno et al., "Leuprorelin rescues polyglutamine-dependent phenotypes in a transgenic mouse model of spinal and bulbar muscular atrophy (SBMA)" Nat. Med. 9: 768–773, 2003. Fig. 3 is reproduced from Waza et al., "17-AAG, an Hsp90 inhibitor, ameliorates polyglutamine-mediated motor neuron degeneration" Nat. Med. 11: 1088–1095, 2005. This work was supported by a Center-of-Excellence (COE) grant from the Ministry of Education, Culture, Sports, Science and Technology, Japan, and grants from the Ministry of Health, Labour and Welfare, Japan.

## References

Adachi, H., Kume, A., Li, M., Nakagomi, Y., Niwa, H., Do, J., Sang, C., Kobayashi, Y., Doyu, M., Sobue, G., 2001. Transgenic mice with an expanded CAG repeat controlled by the human AR promoter show polyglutamine nuclear inclusions and neuronal dysfunction without neuronal cell death. Hum. Mol. Genet. 10, 1039–1048.

Adachi, H., Katsuno, M., Minamiyama, M., Sang, C., Pagoulatos, G., Angelidis, C., Kusakabe, M., Yoshiki, A., Kobayashi, Y., Doyu, M., Sobue, G., 2003. Heat shock protein 70 chaperone overexpression ameliorates phenotypes of the spinal and bulbar muscular atrophy transgenic mouse model by reducing nuclear-localized mutant androgen receptor protein. J. Neurosci. 23, 2203–2211.

Adachi, H., Katsuno, M., Minamiyama, M., Waza, M., Sang, C., Nakagomi, Y., Kobayashi, Y., Tanaka, F., Doyu, M., Inukai, A., Yoshida, M., Hashizume, Y., Sobue, G., 2005. Widespread nuclear and cytoplasmic accumulation of mutant androgen receptor in SBMA patients. Brain 128, 659–670.

Agrawal, N., Pallos, J., Slepko, N., Apostol, B.L., Bodai, L., Chang, L.W., Chiang, A.S., Thompson, L.M., Marsh, J.L., 2005. Identification of combinatorial drug regimens for treatment of Huntington's disease using *Drosophila*. Proc. Natl. Acad. Sci. U. S. A. 102, 3777–3781.

Arrasate, M., Mitra, S., Schweitzer, E.S., Segal, M.R., Finkbeiner, S., 2004. Inclusion body formation reduces levels of mutant huntingtin and the risk of neuronal death. Nature 431, 805–810.

Bailey, C.K., Andriola, I.F., Kampinga, H.H., Merry, D.E., 2002. Molecular chaperones enhance the degradation of expanded polyglutamine repeat androgen receptor in a cellular model of spinal and bulbar muscular atrophy. Hum. Mol. Genet. 11, 515–523.

Banno, H., Adachi, H., Katsuno, M., Suzuki, K., Atsuta, N., Watanabe, H., Tanaka, F., Doyu, M., Sobue, G., in press. Mutant androgen receptor accumulation in SBMA scrotal skin: a pathogenic marker. Ann. Neurol.

Batulan, Z., Shinder, G.A., Minotti, S., He, B.P., Doroudchi, M.M., Nalbantoglu, J., Strong, M.J., Durham, H.D., 2003. High threshold for induction of the stress response in motor neurons is associated with failure to activate HSF1. J. Neurosci. 23, 5789–5798.

Caplen, N.J., Taylor, J.P., Statham, V.S., Tanaka, F., Fire, A., Morgan, R.A., 2002. Rescue of polyglutamine-mediated cytotoxicity by double-stranded RNA-mediated RNA interference. Hum. Mol. Genet. 11, 175–184.

Chevalier-Larsen, E.S., O'Brien, C.J., Wang, H., Jenkins, S.C., Holder, L., Lieberman, A.P., Merry, D.E., 2004. Castration restores function and neurofilament alterations of aged symptomatic males in a transgenic mouse model of spinal and bulbar muscular atrophy. J. Neurosci. 24, 4778–4786.

Clark, P.E., Irvine, R.A., Coetzee, G.A., 2003. The androgen receptor CAG repeat and prostate cancer risk. Methods Mol. Med. 81, 255–266.

Cowan, K.J., Diamond, M.I., Welch, W.J., 2003. Polyglutamine protein aggregation and toxicity are linked to the cellular stress response. Hum. Mol. Genet. 12, 1377–1391.

Doyu, M., Sobue, G., Mukai, E., Kachi, T., Yasuda, T., Mitsuma, T., Takahashi, A., 1992. Severity of X-linked recessive bulbospinal neuronopathy correlates with size of the tandem CAG repeat in androgen receptor gene. Ann. Neurol. 32, 707–710.

Fischbeck, K.H., 1997. Kennedy disease. J. Inherited Metab. Dis. 20, 152–158.

Gatchel, J.R., Zoghbi, H.Y., 2005. Diseases of unstable repeat expansion: mechanism and principles. Nat. Rev., Genet. 6, 743–755.

Gunawardena, S., Goldstein, L.S., 2005. Polyglutamine diseases and transport problems: deadly traffic jams on neuronal highways. Arch. Neurol. 62, 46–51.

Hafezparast, M., Klocke, R., Ruhrberg, C., Marquardt, A., Ahmad-Annuar, A., Bowen, S., Lalli, G., Witherden, A.S., Hummerich, H., Nicholson, S., Morgan, P.J., Oozageer, R., Priestley, J.V., Averillm, S., King, V.R., Ball, S., Peters, J., Toda, T., Yamamoto, A., Hiraoka, Y., Augustin, M., Korthaus, D., Wattler, S., Wabnitz, P., Dickneite, C., Lampel, S., Boehme, F., Peraus, G., Popp, A., Rudelius, M., Schlegel, J., Fuchs, H., Hrabe de Angelis, M., Schiavo, G., Shima, D.T., Russ, A.P., Stumm, G., Martin, J.E., Fisher, E.M., 2003. Mutations in dynein link motor neuron degeneration to defects in retrograde transport. Science 300, 808–812.

Hay, D.G., Sathasivam, K., Tobaben, S., Stahl, B., Marber, M., Mestril, R., Mahal, A., Smith, D.L., Woodman, B., Bates, G.P., 2004. Progressive decrease in chaperone protein levels in a mouse model of Huntington's disease and induction of stress proteins as a therapeutic approach. Hum. Mol. Genet. 13, 1389–1405.

Heinlein, C.A., Chang, C., 2001. Role of chaperones in nuclear translocation and transactivation of steroid receptors. Endocrine 14, 143–149.

Hirakawa, T., Rokutan, K., Nikawa, T., Kishi, K., 1996. Geranylgeranylacetone induces heat shock proteins in cultured guinea pig gastric mucosal cells and rat gastric mucosa. Gastroenterology 111, 345–357.

Hockly, E., Richon, V.M., Woodman, B., Smith, D.L., Zhou, X., Rosa, E., Sathasivam, K., Ghazi-Noori, S., Mahal, A., Lowden, P.A., Steffan, J.S., Marsh, J.L., Thompson, L.M., Lewis, C.M., Marks, P.A., Bates, G.P., 2003. Suberoylanilide hydroxamic acid, a histone deacetylase inhibitor, ameliorates motor deficits in a mouse model of Huntington's disease. Proc. Natl. Acad. Sci. U. S. A. 100, 2041–2046.

Katsuno, M., Adachi, H., Kume, A., Li, M., Nakagomi, Y., Niwa, H., Sang, C., Kobayashi, Y., Doyu, M., Sobue, G., 2002. Testosterone reduction prevents phenotypic expression in a transgenic mouse model of spinal and bulbar muscular atrophy. Neuron 35, 843–854.

Katsuno, M., Adachi, H., Doyu, M., Minamiyama, M., Sang, C., Kobayashi, Y., Inukai, A., Sobue, G., 2003. Leuprorelin rescues polyglutamine-dependent phenotypes in a transgenic mouse model of spinal and bulbar muscular atrophy. Nat. Med. 9, 768–773.

Katsuno, M., Adachi, H., Tanaka, F., Sobue, G., 2004. Spinal and bulbar muscular atrophy: ligand-dependent pathogenesis and therapeutic perspectives. J. Mol. Med. 82, 298–307.

Katsuno, M., Sang, C., Adachi, H., Minamiyama, M., Waza, M., Tanaka, F., Doyu, M., Sobue, G., 2005. Pharmacological induction of heat-shock proteins alleviates polyglutamine-mediated motor neuron disease. Proc. Natl. Acad. Sci. U. S. A. 102, 16801–16806.

Kawahara, H., 1897. A family of progressive bulbar palsy. Aichi. Med. J. 16, 3–4 (in Japanese).

Kennedy, W.R., Alter, M., Sung, J.H., 1968. Progressive proximal spinal and bulbar muscular atrophy of late onset. A sex-linked recessive trait. Neurology 18, 671–680.

Kobayashi, Y., Miwa, S., Merry, D.E., Kume, A., Mei, L., Doyu, M., Sobue, G., 1998. Caspase-3 cleaves the expanded androgen receptor protein of spinal and bulbar muscular atrophy in a polyglutamine repeat length-dependent manner. Biochem. Biophys. Res. Commun. 252, 145–150.

Kobayashi, Y., Kume, A., Li, M., Doyu, M., Hata, M., Ohtsuka, K., Sobue, G., 2000. Chaperones Hsp70 and Hsp40 suppress aggregate formation and apoptosis in cultured neuronal cells expressing truncated androgen receptor protein with expanded polyglutamine tract. J. Biol. Chem. 275, 8772–8778.

La Spada, A.R., Wilson, E.M., Lubahn, D.B., Harding, A.E., Fischbeck, K.H., 1991. Androgen receptor gene mutations in X-linked spinal and bulbar muscular atrophy. Nature 352, 77–79.

Li, M., Miwa, S., Kobayashi, Y., Merry, D.E., Yamamoto, M., Tanaka, F., Doyu, M., Hashizume, Y., Fischbeck, K.H., Sobue, G., 1998. Nuclear inclusions of the androgen receptor protein in spinal and bulbar muscular atrophy. Ann. Neurol. 44, 249–254.

Macario, A.J., Conway de Macario, E., 2005. Sick chaperones, cellular stress, and disease. N. Engl. J. Med. 353, 1489–1501.

Mariotti, C., Castellotti, B., Pareyson, D., Testa, D., Eoli, M., Antozzi, C., Silani, V., Marconi, R., Tezzon, F., Siciliano, G., Marchini, C., Gellera, C., Donato, S.D., 2000. Phenotypic manifestations associated with CAG-repeat expansion in the androgen receptor gene in male patients and heterozygous females: a clinical and molecular study of 30 families. Neuromuscul. Disord. 10, 391–397.

Minamiyama, M., Katsuno, M., Adachi, H., Waza, M., Sang, C., Kobayashi, Y., Tanaka, F., Doyu, M., Inukai, A., Sobue, G., 2004. Sodium butyrate ameliorates phenotypic expression in a transgenic mouse model of spinal and bulbar muscular atrophy. Hum. Mol. Genet. 13, 1183–1192.

Muchowski, P.J., Wacker, J.L., 2005. Modulation of neurodegeneration by molecular chaperones. Nat. Rev., Neurosci. 6, 11–22.

Nucifora Jr., F.C., Sasaki, M., Peters, M.F., Huang, H., Cooper, J.K., Yamada, M., Takahashi, H., Tsuji, S., Troncoso, J., Dawson, V.L., Dawson, T.M., Ross, C. A., 2001. Interference by huntingtin and atrophin-1 with cbp-mediated transcription leading to cellular toxicity. Science 291, 2423–2428.

Poletti, A., 2004. The polyglutamine tract of androgen receptor: from functions to dysfunctions in motor neurons. Front. Neuroendocrinol. 25, 1–26.

Pratt, W.B., Toft, D.O., 2003. Regulation of signaling protein function and trafficking by the hsp90/hsp70-based chaperone machinery. Exp. Biol. Med. 228, 111–133.

Puls, I., Jonnakuty, C., LaMonte, B.H., Holzbaur, E.L., Tokito, M., Mann, E., Floeter, M.K., Bidus, K., Drayna, D., Oh, S.J., Brown Jr., R.H., Ludlow, C.L., Fischbeck, K.H., 2003. Mutant dynactin in motor neuron disease. Nat. Genet. 33, 455–456.

Schmidt, B.J., Greenberg, C.R., Allingham-Hawkins, D.J., Spriggs, E.L., 2002. Expression of X-linked bulbospinal muscular atrophy (Kennedy disease) in two homozygous women. Neurology 59, 770–772.

Sobue, G., Hashizume, Y., Mukai, E., Hirayama, M., Mitsuma, T., Takahashi, A., 1989. X-linked recessive bulbospinal neuronopathy. A clinicopathological study. Brain 112, 209–232.

Sobue, G., Doyu, M., Kachi, T., Yasuda, T., Mukai, E., Kumagai, T., Mitsuma, T., 1993. Subclinical phenotypic expressions in heterozygous females of X-linked recessive bulbospinal neuronopathy. J. Neurol. Sci. 117, 74–78.

Sopher, B.L., Thomas, Jr., P.S., LaFevre-Bernt, M.A., Holm, I.E., Wilke, S.A., Ware, C.B., Jin, L.W., Libby, R.T., Ellerby, L.M., La Spada, A.R., 2004. Androgen receptor YAC transgenic mice recapitulate SBMA motor neuronopathy and implicate VEGF164 in the motor neuron degeneration. Neuron 41, 687–699.

Sperfeld, A.D., Karitzky, J., Brummer, D., Schreiber, H., Haussler, J., Ludolph, A.C., Hanemann, C.O., 2002. X-linked bulbospinal neuropathy: Kennedy disease. Arch. Neurol. 59, 1921–1926.

Steffan, J.S., Bodai, L., Pallos, J., Poelman, M., McCampbell, A., Apostol, B.L., Kazantsev, A., Schmidt, E., Zhu, Y.Z., Greenwald, M., Kurokawa, R., Housman, D.E., Jackson, G.R., Marsh, J.L., Thompson, L.M., 2001. Histone deacetylase inhibitors arrest polyglutamine-dependent neurodegeneration in *Drosophila*. Nature 413, 739–743.

Sugars, K.L., Rubinsztein, D.C., 2003. Transcriptional abnormalities in Huntington disease. Trends Genet. 19, 233–238.

Szebenyi, G., Morfini, G.A., Babcock, A., Gould, M., Selkoe, K., Stenoien, D.L., Young, M., Faber, P.W., MacDonald, M.E., McPhaul, M.J., Brady, S.T., 2003. Neuropathogenic forms of huntingtin and androgen receptor inhibit fast axonal transport. Neuron 40, 41–52.

Takeyama, K., Ito, S., Yamamoto, A., Tanimoto, H., Furutani, T., Kanuka, H., Miura, M., Tabata, T., Kato, S., 2002. Androgen-dependent neurodegeneration by polyglutamine-expanded human androgen receptor in *Drosophila*. Neuron 35, 855–864.

Walcott, J.L., Merry, D.E., 2002. Ligand promotes intranuclear inclusions in a novel cell model of spinal and bulbar muscular atrophy. J. Biol. Chem. 277, 50855–50859.

Waza, M., Adachi, H., Katsuno, M., Minamiyama, M., Sang, C., Tanaka, F., Inukai, A., Doyu, M., Sobue, G., 2005. 17-AAG, an Hsp90 inhibitor, ameliorates polyglutamine-mediated motor neuron degeneration. Nat. Med. 11, 1088–1095.

Wyttenbach, A., 2004. Role of heat shock proteins during polyglutamine neurodegeneration: mechanisms and hypothesis. J. Mol. Neurosci. 23, 69–96.

# Mutant Androgen Receptor Accumulation in Spinal and Bulbar Muscular Atrophy Scrotal Skin: A Pathogenic Marker

Haruhiko Banno, MD, Hiroaki Adachi, MD, Masahisa Katsuno, MD, Keisuke Suzuki, MD, Naoki Atsuta, MD, Hirohisa Watanabe, MD, Fumiaki Tanaka, MD, Manabu Doyu, MD, and Gen Sobue, MD

***Objective:*** **Spinal and bulbar muscular atrophy (SBMA) is a hereditary motor neuron disease caused by the expansion of a polyglutamine tract in the androgen receptor (AR). The nuclear accumulation of mutant AR is central to the pathogenesis of SBMA. Androgen deprivation with leuprorelin inhibits mutant AR accumulation, resulting in rescue of neuronal dysfunction in a mouse model of SBMA. This study aimed to investigate whether mutant AR accumulation in the scrotal skin is an appropriate biomarker of SBMA.** ***Methods:*** **Immunohistochemistry of both scrotal skin and the spinal cord was performed on five autopsied SBMA cases. Neurological severity and scrotal skin findings were studied in another 13 patients. Five other patients received subcutaneous injections of leuprorelin and underwent scrotal skin biopsy.** ***Results:*** **The degree of mutant AR accumulation in scrotal skin epithelial cells tended to be correlated with that in the spinal motor neurons in autopsy specimens, and it was well correlated with CAG repeat length and inversely correlated with the amyotrophic lateral sclerosis functional scale. Leuprorelin treatment inhibited mutant AR protein accumulation in the scrotal skin of SBMA patients.** ***Interpretation:*** **These observations suggest that scrotal skin biopsy findings are a potent pathogenic marker of SBMA and can be a surrogate end point in therapeutic trials.**

Ann Neurol 2006;59:520–526

Spinal and bulbar muscular atrophy (SBMA), also known as Kennedy's disease, is an adult-onset motor neuron disease characterized by muscle atrophy, weakness, contraction fasciculations, and bulbar involvement.[1–4] SBMA exclusively affects men in their 30s or 40s, and disease progression is slow.[1,5] The molecular basis of SBMA is the expansion of a trinucleotide CAG repeat, which encodes a polyglutamine (polyQ) tract, in the androgen receptor (AR) gene.[6] The CAG repeat numbers range from 38 to 62 in SBMA patients, whereas healthy individuals have 10 to 36 CAGs.[6,7] The number of CAGs is correlated with disease severity and is inversely correlated with age of onset,[8,9] as observed in other polyQ-related neurodegenerative diseases including Huntington's disease and several forms of spinocerebellar ataxia.[10]

Histopathologically, lower motor neurons are markedly depleted in the spinal cord and brainstem, and nuclear inclusions (NIs) containing the mutant and truncated AR with expanded polyQ are present in the residual motor neurons, as well as in cells of the scrotal skin and other visceral organs.[3,11,12] Although NIs are a disease-specific pathological marker, they may reflect a cellular protective response against the toxicity of abnormal polyQ-containing protein.[13] In contrast, the therapeutic effect of testosterone deprivation in our SBMA transgenic mouse model suggested that diffuse nuclear accumulation of mutant AR is a cardinal pathogenic process underlying neurological manifestations.[14,15] This hypothesis has also been clearly illustrated by the observation that the extent of diffuse nuclear accumulation of mutant AR, but not NIs, in the motor neurons of the spinal cord was closely related to CAG repeat length in autopsied SBMA cases.[16] Nuclear localization of the mutant protein has now been considered essential for inducing neuronal cell dysfunction and degeneration in the majority of polyQ diseases.[10]

A characteristic clinical feature of SBMA is that the disease occurs in male but not female individuals, even when they are homozygous for the mutation.[17,18] Several studies have clarified that the sex dependency of disease manifestation in SBMA arises from testosterone-dependent nuclear accumulation of mu-

From the Department of Neurology, Nagoya University Graduate School of Medicine, Showa-ku, Nagoya, Japan.

Received Sep 1, 2005, and in revised form Oct 4. Accepted for publication Oct 6, 2005.

Published online Dec 15, 2005 in Wiley InterScience (www.interscience.wiley.com). DOI: 10.1002/ana.20735

Address correspondence to Dr Sobue, Department of Neurology, Nagoya University Graduate School of Medicine, 65 Tsurumai-cho, Showa-ku, Nagoya 466-8550, Japan.
E-mail: sobueg@med.nagoya-u.ac.jp

 

tant AR.[14,15,19,20] Leuprorelin, a leuteinizing hormone–releasing hormone agonist that reduces testosterone release from the testis and inhibits nuclear accumulation of mutant AR, rescued motor dysfunction in male transgenic mice carrying the full-length human AR with expanded polyQ.[15]

Although data from transgenic mice studies indicated that androgen deprivation from leuprorelin treatment is a potent therapeutic agent for SBMA,[14,15] clinical experience using this drug for SBMA patients is limited.[21] Because long-term clinical trials are needed to establish the efficacy of therapeutics ameliorating disease progression in slowly progressive neurodegenerative diseases such as SBMA, an appropriate biomarker reflecting pathogenic processes of the disease is necessary. The aim of this study was to test the hypothesis that peripheral accumulation of mutant AR in the scrotal skin represents a suitable biomarker of SBMA that can be applicable as a surrogate end point in therapeutic trials.

## Patients and Methods

### *Patients*

Twenty-three patients with clinically and genetically confirmed SBMA were examined. Patient characteristics are shown in the Table. Five of the 23 patients underwent autopsy, and both the scrotal skin and the spinal cord were examined; another 13 patients underwent biopsy of the scrotal skin. The remaining five patients were enrolled in a leuprorelin study and also underwent biopsy of the scrotal skin. All patients were hospitalized and underwent follow-up examinations at Nagoya University Hospital (Nagoya, Japan) and its affiliated hospitals.

For each of the 18 patients who underwent biopsy of the scrotal skin, three scrotal skin specimens were made by punch biopsy using a 3mm diameter Dermapunch (Nipro, Tokyo, Japan) under 10ml lidocaine acetate local anesthesia. All patients who underwent biopsy sterilized the wound for several days by themselves and received 4 days of cefaclor (250mg three times a day) antibiotic therapy after the procedure. The 13 patients who underwent biopsy who were not enrolled in the leuprorelin trial were also assessed on the amyotrophic lateral sclerosis functional scale (limb Norris score), as described previously.[22]

Five other male subjects (age, 60–74 years; mean, 67.3 years) who died of nonneurological diseases served as control subjects. The Nagoya University Hospital Institutional Review Board approved the collection of data and specimens, and all patients gave their written, informed consent to participate.

### *Leuprorelin Administration*

Five patients received subcutaneous injections of 3.75mg leuprorelin once every 4 weeks. The patients, aged 43 to 68 years, were capable of walking with or without a cane and expressed no desire to father a child. They were observed for 6 months (24 weeks), and scrotal skin biopsies were taken from each patient at 0, 4, and 12 weeks after initial leuprorelin administration. Serum creatine kinase (CK) was determined by ultraviolet measurement using hexokinase and glucose-6-phosphate. Serum testosterone levels were measured by radioimmunoassay using the DPC total testosterone kit (Diagnostic Products Corporation, Los Angeles, CA).

### *Immunohistochemical Detection of the Mutant Androgen Receptor in the Scrotal Skin and Spinal Cord*

Immunohistochemistry of scrotal skin specimens and the spinal cord were conducted as described previously.[16] In brief, we prepared 5μm-thick, formalin-fixed, paraffin-embedded sections of scrotal skin and spinal cord from SBMA patients. Sections were deparaffinized and rehydrated through a graded series of alcohol-water solutions. For the mutant AR immunohistochemical study, sections were pretreated with immersion in 98% formic acid for 5 minutes, and then with microwave oven heating for 15 minutes in 10mM citrate buffer at pH 6.0. Sections were incubated with a mouse anti-expanded polyQ antibody (1:20,000; 1C2; Chemicon, Temecula, CA)[23] to evaluate the nuclear accumulation of mutant AR.[14–16] Immune complexes were visualized using the Envision-plus kit (Dako, Glostrup, Denmark). Sections were counterstained with Mayer's hematoxylin. For electron microscopic immunohistochemistry, the sections were processed

*Table. Patient Characteristics*

| Characteristics | Autopsy Study (N = 5) | Biopsy Alone Study (N = 13) | Leuprorelin + Biopsy Study (N = 5) |
|---|---|---|---|
| Age (mean ± SD), yr | 64.8 ± 10.8 | 54.8 ± 9.6 | 50.2 ± 10.8 |
| Duration of weakness (mean ± SD), yr | 38.4 ± 14.7 | 11.0 ± 7.4 | 8.8 ± 4.9 |
| (CAG)n (mean ± SD) | 47.4 ± 4.9 | 48.2 ± 3.0 | 49.2 ± 4.9 |
| ADL (cane/independent ratio) | NA | 4/9 | 2/3 |
| Limb Norris score (mean ± SD) | NA | 53.4 ± 6.9 | 52.0 ± 6.8 |
| Norris bulbar score (mean ± SD) | NA | 32.2 ± 3.4 | 32.8 ± 6.2 |
| ALSFRS-R (Japanese edition) (mean ± SD) | NA | 40.3 ± 3.2 | 39.2 ± 3.8 |
| Cause of death | Pneumonia (n = 4); Lung cancer (n = 1) | NA | NA |

The amyotrophic lateral sclerosis functional rating scale-revised.
SD = standard deviation; (CAG)n = number of expanded CAG repeats in the SBMA allele; NA = not applicable; ADL = activities of daily living.

as described for light microscopic immunohistochemistry, and then fixed with 2% osmium tetroxide in 0.1M phosphate buffer at pH 7.4, dehydrated in graded alcohol-water solutions, and embedded in epoxy resin. Ultrathin sections were cut for observation under an electron microscope (H-7100; Hitachi High-Technologies Corporation, Tokyo, Japan).

### *Quantification of Cell Population with Diffuse Nuclear Staining*

For quantitative assessment of scrotal skin cells, the frequency of diffuse nuclear staining was calculated from counts of more than 500 nuclei in 5 randomly selected fields of each section photographed at 400× magnification (BX51TF; Olympus, Tokyo, Japan). To assess the nuclear accumulation of mutant AR in spinal cord motor neurons, we prepared at least 100 transverse sections each from the cervical, thoracic, and lumber spinal cord for anti-expanded polyQ antibody staining with 1C2. The numbers of 1C2-positive cells in the ventral horn on both the right and left sides were counted on every 10th section under the light microscope with a computer-assisted image analyzer (BX51TF; Olympus), as described previously.[16,24] Populations of 1C2-positive cells were expressed as percentages of the total skin cell or neuronal count.

### *Statistical Analysis*

We analyzed the data by Pearson's coefficient, Spearman's rank correlation, and Student's paired $t$ test as appropriate using StatView software (version 5; Hulinks, Tokyo, Japan) and considering $p$ values less than 0.05 to be indicative of significance.

## Results

### *Mutant Androgen Receptor Nuclear Accumulation in the Scrotal Skin and Spinal Motor Neuron*

In the five autopsied cases, mutant AR nuclear accumulations were clearly visualized with anti-expanded polyQ immunostaining with 1C2 in the scrotal skin and spinal cord specimens (Fig 1A). Pathological accumulation of mutant AR was distributed in all layers of the epithelium. Diffuse nuclear accumulations were predominantly observed, and the occurrence of NIs was less frequent. This was also the case in the spinal cord specimens. Electron microscopic immunohistochemistry with the 1C2 antibody demonstrated granular dense and amorphous aggregates corresponding to diffuse nuclear staining in both spinal motor neurons and epithelial cells of scrotal skin (see Figs 1B, C). Filamentous structures such as those reported in Huntington's disease,[25] dentatorubal-pallidoluysian atrophy (DRPLA),[26] and Machado–Joseph disease[27] were not seen. No diffuse nuclear staining was seen in the control subjects. The extent of mutant AR accumulation in the scrotal skin epithelial cells showed a tendency to correlate with that in the anterior horn cells ($r = 0.84$; $p = 0.08$; see Fig 1D). Mutant AR accumulation was remarkable in both the spinal motor neurons and the scrotal skin of Patient 1, but was far less remarkable in Patient 2 (see Figs 1A, D).

### *Correlations of the Mutant Androgen Receptor Accumulation in the Scrotal Skin to CAG Repeat Length and Amyotrophic Lateral Sclerosis Score*

Mutant AR nuclear accumulations in scrotal skin biopsies from the 13 SBMA patients who did not receive leuprorelin were assessed by 1C2 antibody staining of expanded PolyQ. The 1C2-positive cell population in the scrotal skin biopsies was significantly correlated with CAG repeat length ($r = 0.61$; $p = 0.03$; Fig 2A) and was inversely correlated with the functional scale assessed by the Norris score on limbs ($r = -0.63$; $p = 0.02$; see Fig 2B).

### *Leuprorelin Treatment Depletes Mutant Androgen Receptor Accumulation in the Scrotal Skin*

In all five patients in which leuprorelin was administered (see the Table), both the intensity and the frequency of diffuse nuclear 1C2 staining in the scrotal epithelial cells was decreased after the first 4 weeks of administration compared with the preadministration values, and this effect was markedly enhanced after 12 weeks of treatment (Figs 3A, B). Quantitative analysis demonstrated a significant decrease in the frequency of 1C2-positive cells both 4 and 12 weeks after the initiation of leuprorelin treatment ($p < 0.01$) (see Fig 3C). Serum testosterone levels decreased to the castration level after 1 to 2 months of treatment (see Fig 3D), and serum CK values were also significantly decreased in all patients (see Fig 3D).

None of the patients showed the hot flush or obesity often reported in leuprorelin trials for prostate cancer. Although a loss of sexual function including erectile disorder was observed in all patients, no patients experienced depression. No marked exacerbations were observed in total cholesterol, triglyceride, fasting blood sugar, or HbA1c (data not shown). We could not find significant motor function changes assessed by amyotrophic lateral sclerosis functional scores in 24 weeks, but three of the five enrolled patients expressed apparent subjective improvement.

## Discussion

This study demonstrated that scrotal skin biopsy with anti-expanded polyQ staining is a strong candidate for an appropriate biomarker with which to monitor SBMA pathogenic processes. Previous studies showed that the severity and progression of motor dysfunction and abatement of abnormalities in mice that were castrated or given leuprorelin paralleled the extent of diffuse nuclear mutant AR accumulation in their spinal motor neurons.[14,15] Furthermore, we demonstrated previously a significant, close correlation between the length of CAG repeat expansion and frequency of dif-

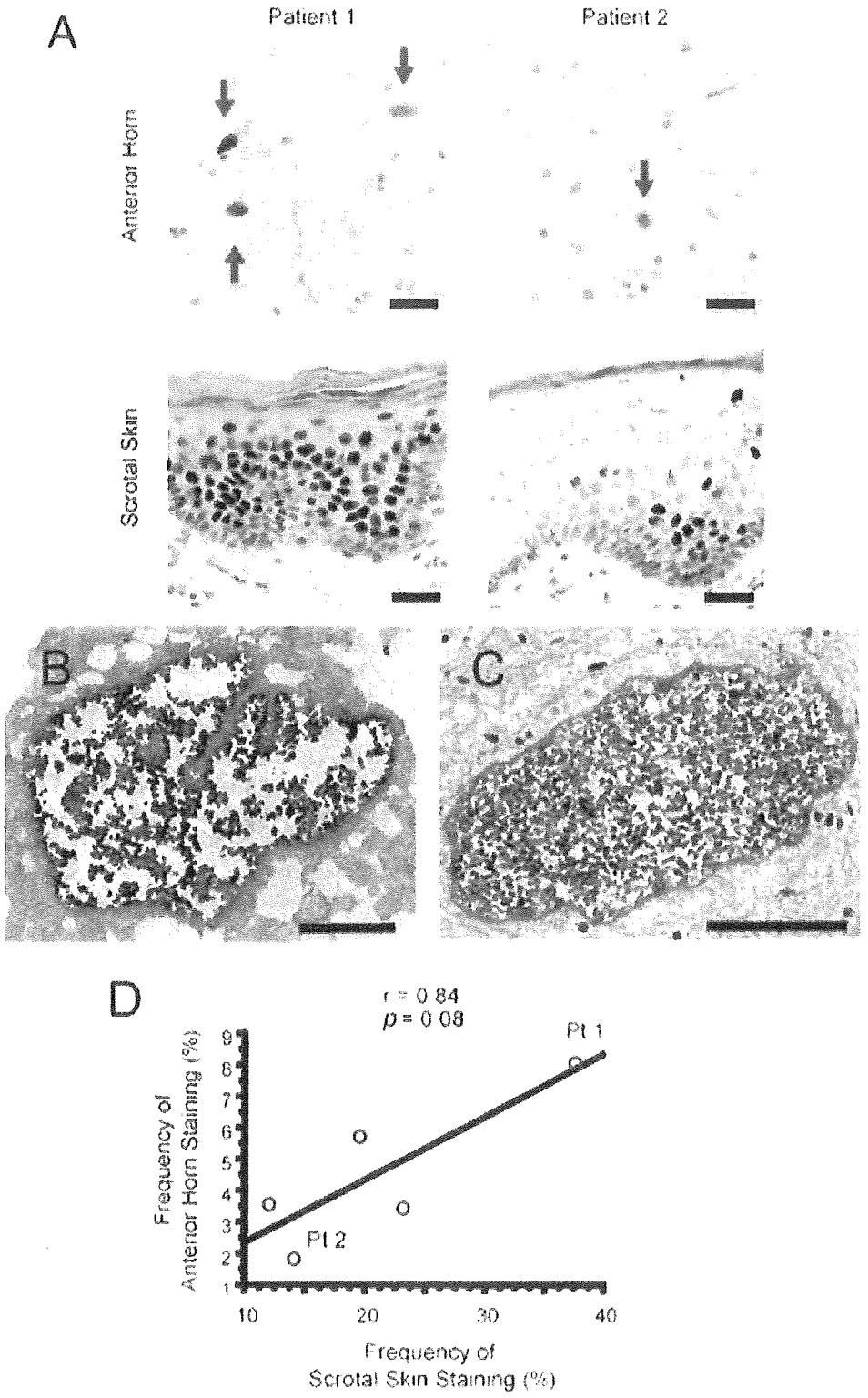


*Fig 1. Mutant androgen receptor (AR) nuclear accumulation in scrotal skin and spinal motor neurons. (A) Mutant AR accumulation was remarkable in both spinal motor neurons (arrows) and scrotal skin of Patient 1, but was less remarkable in both motor neurons (arrows) and skin in Patient 2. Bar = 30μm. (B, C) Electron microscopic immunohistochemistry for 1C2 demonstrated granular dense and amorphous aggregates corresponding to diffuse nuclear staining in both spinal motor neurons and epithelial cells of scrotal skin. Bar =3μm. (D) The extent of mutant AR accumulation in scrotal skin epithelial cells showed a tendency to correlate with that in anterior horn cells. Circles (Pt. 1, Pt. 2) correspond to Patient 1 and 2 in Fig 1A.*

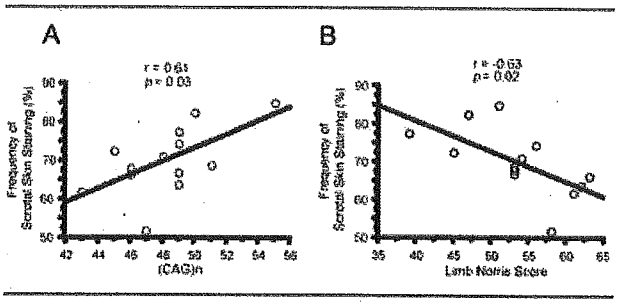


*Fig 2. Correlation of the frequency of scrotal skin staining to CAG repeats and limb Norris score. The frequency of 1C2-positive cells in the scrotal skin biopsies correlated significantly with (A) CAG repeat length and (B) inversely correlated with the amyotrophic lateral sclerosis functional scale assessed by the Norris score on limbs. (CAG)n = number of expanded CAG repeats in the spinal and bulbar muscular atrophy allele.*

fuse nuclear mutant AR accumulation, but not that of NIs, in the spinal cord.[16] Accordingly, neuronal dysfunction is likely to be caused by diffuse nuclear accumulation of mutant AR in the affected tissues. In this study, the extent of mutant AR nuclear accumulation in scrotal skin cells paralleled that in the anterior horn cells in autopsied cases. Electron microscopic immunohistochemistry for 1C2 anti-expanded PolyQ demonstrated granular dense and amorphous aggregates corresponding to diffuse nuclear staining in both spinal motor neurons and epithelial cells of scrotal skin. Furthermore, the fine structure of the aggregates in spinal motor neurons and epithelial cells was quite similar. Biopsy analyses in this study also suggested that scrotal skin findings were correlated with the motor functional scores of SBMA patients.

Our findings suggest that nuclear mutant AR assessed by 1C2 immunostaining in the scrotal skin is a practical procedure to estimate the severity of SBMA pathogenesis in the nervous system. In support of this view, decreases in mutant AR accumulation in the motor neurons paralleled that in nonneuronal cells in the androgen deprivation therapy tested in the mouse model of SBMA. In addition, leuprorelin treatment markedly reduced serum testosterone levels, as well as nuclear accumulation of mutant AR in the scrotal skin, suggesting that medical castration with leuprorelin intervenes in the pathogenic process of human SBMA, as demonstrated in the animal study. Moreover, serum CK levels were significantly decreased in this leuprorelin study. Because high CK values are common in SBMA patients and histopathological examinations have shown myogenic changes together with neurogenic findings in this disease,[1,3] presumably, a decrease in CK values with leuprorelin treatment implies muscular protection. Serum CK levels, however, did not significantly correlate with the Norris score on limbs or with scrotal skin biopsy findings in our cross-sectional study.

As defined by the Biomarkers Definitions Working Group, a disease biomarker should be objectively measurable and evaluated as an indicator of pathogenic processes or pharmacological responses to a therapeutic intervention.[28] Based on the observations described earlier, 1C2-stained mutant AR accumulation in the biopsied scrotal skin is likely to be a potent biomarker reflecting pathogenic processes of SBMA. Particularly, the correlation of the extent of mutant AR nuclear accumulation in the spinal motor neurons with that in scrotal skin biopsies in the autopsied cases suggests that findings in the scrotal skin can predict pathogenic processes in the motor neurons.

Although its precise natural history has not been evaluated, SBMA is a slowly progressive disease.[1,5] Thus, extremely long-term clinical trials are necessary to assess whether certain drugs can alter the natural disease progression by targeting clinical end points such as occurrence of aspiration pneumonia or becoming wheelchair bound. Suitable surrogate end points, which reflect the pathogenesis and severity of SBMA, are substantial to assess the therapeutic efficacy in drug trials. Although it is not practical to obtain biopsy specimens from the central nervous system (CNS), a punch biopsy of the scrotal skin enables a safe and accessible examination for patients.

It has also been suggested that reliance on surrogate end points can be misleading because they may not accurately predict the actual effects that treatments have on the health of a patient, as was seen with the CD4 counts in human immunodeficiency virus trials, the bone mineral density in osteoporosis trials, and others.[29] However, several factors have been suggested to consider the decision to rely on a surrogate.[30] In SBMA, mutant AR accumulation assessed by scrotal skin biopsy can be a candidate for a surrogate end point in light of several pieces of evidence. First, a credible SBMA animal model demonstrated dramatic functional motor recovery in response to testosterone deprivation therapy that depleted mutant AR accumulation in the central nervous system, as well as in nonneuronal tissues.[14,15] Second, the degree of diffuse nuclear accumulation of mutant AR in both the CNS and scrotal skin correlates well with CAG repeat length and disease severity, indicating that it is a natural phenomenon of and reflects the underlying pathology of the disease. Third, autopsy studies show that levels of nuclear AR accumulation in the scrotal skin are correlated with those in the CNS. Moreover, levels of nuclear translocated mutant AR in the scrotal skin decreased significantly in response to drug therapy that has been shown to deplete such accumulations in the CNS of SBMA mice, to significantly rescue motor dysfunction in these mice, and to partially stabilize neurological symptoms in one reported case of human SBMA.[21]

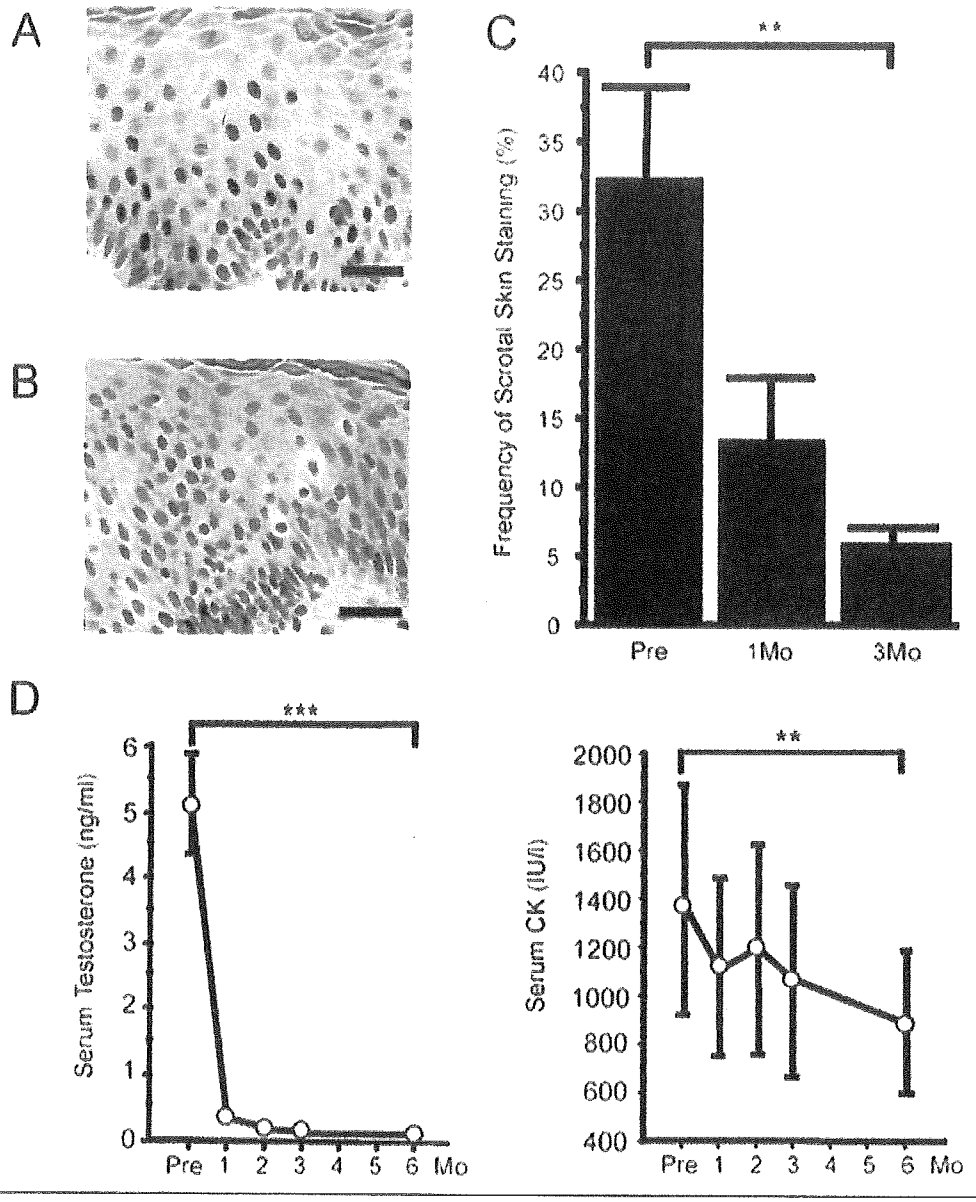


*Fig 3. Effects of leuprorelin on mutant androgen receptor (AR) accumulation in scrotal skin, serum testosterone, and creatine kinase (CK). (A) Scrotal skin shows intense and frequent staining for anti-polyglutamine antibody in the nucleus before therapy. (B) Twelve weeks after therapy, both intensity and frequency of nuclear staining markedly decreased. Bar = 30μm. (C) Quantitative analysis of immunohistochemistry demonstrated a significant decrease in the number of positively stained nuclei. (D) Serum testosterone and CK decreased significantly in 6 months. Frequency of staining was calculated from counts of more than 500 nuclei in randomly selected areas and was expressed as mean ± standard deviation for 5 patients.* $^{**}p < 0.01$; $^{***}p < 0.0001$.

Although our results were obtained from a small sample, nuclear accumulation of mutant AR in the scrotal skin appears to be a potent pathogenic biomarker of SBMA. A correlation between decline in validated clinical scales and nuclear mutant AR accumulations must be demonstrated in a longitudinal study to verify this histopathological feature as a biomarker for clinical severity. Similarly, validation of the scrotal skin biopsy findings as a surrogate end point in clinical trials will require a longitudinal study verifying that suppression of nuclear staining correlates with improvement on a validated clinical scale and the true clinical outcome events such as the need for a wheelchair, the presence of aspiration pneumonia, or death.

This work was supported by grants from the Ministry of Education, Culture, Sports, Science and Technology, Japan (17204032, G. S., M. D., F. T.); the Ministry of Health, Labor and Welfare, Japan (H-15-Kokoro-020, G. S., M. D.); and the Center for Clinical Trials, Japan Medical Association (G.S.).

We thank Dr N. Hishikawa for technical assistance.

## References


1. Kennedy WR, Alter M, Sung JH. Progressive proximal spinal and bulbar muscular atrophy of late onset: a sex-linked recessive trait. Neurology 1968;18:671–680.
2. Sperfeld AD, Karitzky J, Brummer D, et al. X-linked bulbospinal neuropathy: Kennedy disease. Arch Neurol 2002;59: 1921–1926.
3. Sobue G, Hashizume Y, Mukai E, et al. X-linked recessive bulbospinal neuronopathy: a clinicopathological study. Brain 1989; 112:209–232.
4. Katsuno M, Adachi H, Tanaka F, et al. Spinal and bulbar muscular atrophy (SBMA): ligand-dependent pathogenesis and therapeutic perspective. J Mol Med 2004;82:298–307.
5. Sobue G, Adachi H, Katsuno M. Spinal and bulbar muscular atrophy (SBMA). In: Dickinson D, ed. Neurodegeneration: the molecular pathology of dementia and movement disorders. Basel: INS Neuropathology, 2003:275–279.
6. La Spada AR, Wilson EM, Lubahn DB, et al. Androgen receptor gene mutations in X-linked spinal and bulbar muscular atrophy. Nature 1991;352:77–79.
7. Tanaka F, Doyu M, Ito Y, et al. Founder effect in spinal and bulbar muscular atrophy (SBMA). Hum Mol Genet 1996;5: 1253–1257.
8. Doyu M, Sobue G, Mukai E, et al. Severity of X-linked recessive bulbospinal neuronopathy correlates with size of the tandem CAG repeat in androgen receptor gene. Ann Neurol 1992; 32:707–710.
9. Shimada N, Sobue G, Doyu M, et al. X-linked recessive bulbospinal neuronopathy: clinical phenotypes and CAG repeat size in androgen receptor gene. Muscle Nerve 1995;18: 1378–1384.
10. Zoghbi HY, Orr HT. Glutamine repeats and neurodegeneration. Annu Rev Neurosci 2000;23:217–247.
11. Li M, Miwa S, Kobayashi Y, et al. Nuclear inclusions of the androgen receptor protein in spinal and bulbar muscular atrophy. Ann Neurol 1998;44:249–254.
12. Li M, Nakagomi Y, Kobayashi Y, et al. Nonneural nuclear inclusions of androgen receptor protein in spinal and bulbar muscular atrophy. Am J Pathol 1998;153:695–701.
13. Arrasate M, Mitra S, Schweitzer ES, et al. Inclusion body formation reduces levels of mutant huntingtin and the risk of neuronal death. Nature 2004;431:805–810.
14. Katsuno M, Adachi H, Kume A, et al. Testosterone reduction prevents phenotypic expression in a transgenic mouse model of spinal and bulbar muscular atrophy. Neuron 2002;35: 843–854.
15. Katsuno M, Adachi H, Doyu M, et al. Leuprorelin rescues polyglutamine-dependent phenotypes in a transgenic mouse model of spinal and bulbar muscular atrophy. Nat Med 2003; 9:768–773.
16. Adachi H, Katsuno M, Minamiyama M, et al. Widespread nuclear and cytoplasmic accumulation of mutant androgen receptor in SBMA patients. Brain 2005;128:659–670.
17. Sobue G, Doyu M, Kachi T, et al. Subclinical phenotypic expressions in heterozygous females of X-linked recessive bulbospinal neuronopathy. J Neurol Sci 1993;117:74–78.
18. Schmidt BJ, Greenberg CR, Allingham-Hawkins DJ, Spriggs EL. Expression of X-linked bulbospinal muscular atrophy (Kennedy disease) in two homozygous women. Neurology 2002;59:770–772.
19. Takeyama K, Ito S, Yamamoto A, et al. Androgen-dependent neurodegeneration by polyglutamine-expanded human androgen receptor in Drosophila. Neuron 2002;35:855–864.
20. Chevalier-Larsen ES, O'Brien CJ, Wang H, et al. Castration restores function and neurofilament alterations of aged symptomatic males in a transgenic mouse model of spinal and bulbar muscular atrophy. J Neurosci 2004;24:4778–4786.
21. Shimohata T, Kimura T, Nishizawa M, et al. Five year follow up of a patient with spinal and bulbar muscular atrophy treated with leuprorelin. J Neurol Neurosurg Psychiatry 2004;75: 1206–1207.
22. Norris FH Jr, Calanchini PR, Fallat RJ, et al. The administration of guanidine in amyotrophic lateral sclerosis. Neurology 1974;24:721–728.
23. Trottier Y, Lutz Y, Stevanin G, et al. Polyglutamine expansion as a pathological epitope in Huntington's disease and four dominant cerebellar ataxias. Nature 1995;378:403–406.
24. Terao S, Sobue G, Hashizume Y, et al. Age-related changes in human spinal ventral horn cells with special reference to the loss of small neurons in the intermediate zone: a quantitative analysis. Acta Neuropathol (Berl) 1996;92:109–114.
25. DiFiglia M, Sapp E, Chase KO, et al. Aggregation of huntingtin in neuronal intranuclear inclusions and dystrophic neurites in brain. Science 1997;277:1990–1993.
26. Hayashi Y, Kakita A, Yamada M, et al. Hereditary dentatorubral-pallidoluysian atrophy: ubiquitinated filamentous inclusions in the cerebellar dentate nucleus neurons. Acta Neuropathol (Berl) 1998;95:479–482.
27. Paulson HL, Perez MK, Trottier Y, et al. Intranuclear inclusions of expanded polyglutamine protein in spinocerebellar ataxia type 3. Neuron 1997;19:333–344.
28. Biomarkers Definitions Working Group. Biomarkers and surrogate endpoints: preferred definitions and conceptual framework. Clin Pharmacol Ther 2001;69:89–95.
29. Fleming TR, DeMets DL. Surrogate end points in clinical trials: are we being misled? Ann Intern Med 1996;125: 605–613.
30. Temple R. Are surrogate markers adequate to assess cardiovascular disease drugs? JAMA 1999;282:790–795.

Journal of Neuroscience Research 83:119–133 (2006)

# Disease Progression of Human SOD1 (G93A) Transgenic ALS Model Rats

**Arifumi Matsumoto,[1,3,6] Yohei Okada,[1,4,6] Masanori Nakamichi,[5] Masaya Nakamura,[2] Yoshiaki Toyama,[2] Gen Sobue,[4] Makiko Nagai,[3] Masashi Aoki,[3] Yasuto Itoyama,[3] and Hideyuki Okano[1,6]***

[1]Department of Physiology, Keio University School of Medicine, Tokyo, Japan
[2]Department of Orthopaedic Surgery, Keio University School of Medicine, Tokyo, Japan
[3]Department of Neurology, Tohoku University Graduate School of Medicine, Sendai, Japan
[4]Department of Neurology, Nagoya University Graduate School of Medicine, Nagoya, Japan
[5]Takeda Chemical Industries, Ltd., Osaka, Japan
[6]Core Research for Evolutional Science and Technology (CREST), Japan Science and Technology Agency (JST), Saitama, Japan

The recent development of a rat model of amyotrophic lateral sclerosis (ALS) in which the rats harbor a mutated human SOD1 (G93A) gene has greatly expanded the range of potential experiments, because the rats' large size permits biochemical analyses and therapeutic trials, such as the intrathecal injection of new drugs and stem cell transplantation. The precise nature of this disease model remains unclear. We described three disease phenotypes: the forelimb-, hindlimb-, and general-types. We also established a simple, non-invasive, and objective evaluation system using the body weight, inclined plane test, cage activity, automated motion analysis system (SCANET), and righting reflex. Moreover, we created a novel scale, the Motor score, which can be used with any phenotype and does not require special apparatuses. With these methods, we uniformly and quantitatively assessed the onset, progression, and disease duration, and clearly presented the variable clinical course of this model; disease progression after the onset was more aggressive in the forelimb-type than in the hindlimb-type. More importantly, the disease stages defined by our evaluation system correlated well with the loss of spinal motor neurons. In particular, the onset of muscle weakness coincided with the loss of approximately 50% of spinal motor neurons. This study should provide a valuable tool for future experiments to test potential ALS therapies. 

**Key words:** amyotrophic lateral sclerosis; evaluation system; behavioral analyses; phenotype; variability

Amyotrophic lateral sclerosis (ALS) is a fatal neurodegenerative disorder that mainly affects the upper and lower motor neurons (de Belleroche et al., 1995). It is characterized by progressive muscle weakness, amyotrophy, and death from respiratory paralysis, usually within 3–5 years of onset (Brown 1995). Although most cases of ALS are sporadic (SALS), approximately 10% are familial (FALS) (Mulder et al., 1986). Moreover, 20–25% of FALS cases are due to mutations in the gene encoding copper-zinc superoxide dismutase (SOD1) (Deng et al., 1993; Rosen et al., 1993). More than 100 different mutations in the SOD1 gene have been identified in FALS so far.

Until recently, animal models of FALS have been various transgenic mice that express a mutant human SOD1 (hSOD1) gene. Of these, a transgenic mouse carrying the G93A (Gly-93 → Ala) mutant hSOD1 gene was the first described (Gurney et al., 1994) and is used all over the world because this model closely recapitulates the clinical and histopathological features of the human disease. To evaluate the therapeutic effects of potential ALS treatments in this animal, many motor-related behavioral tasks are used (Chiu et al., 1995; Barneoud et al., 1997; Garbuzova-Davis et al., 2002; Sun et al., 2002; Wang et al., 2002; Inoue et al., 2003; Kaspar et al., 2003; Weydt et al., 2003; Azzouz et al., 2004). However, transgenic mice have innate limitations for some types of experiments because of their small size.

Recently, transgenic rat models of ALS, which harbor the hSOD1 gene containing the H46R (His-46 → Arg) or G93A mutation were generated (Nagai et al., 2001). The larger size of these rat models makes certain experiments easier, such as biochemical analyses that require large amounts of sample, intrathecal administration

Contract grant sponsor: Core Research for Evolutional Science and Technology (CREST), Japan Science and Technology Agency (JST); Contract grant sponsor: Japanese Ministry of Health, Labour and Welfare; Contract grant sponsor: Japanese Ministry of Education, Culture, Sports, Science and Technology.

*Correspondence to: Hideyuki Okano, Department of Physiology, School of Medicine, Keio University, 35 Shinanomachi, Shinjuku-ku, Tokyo, 160-8582, Japan. E-mail: hidokano@sc.itc.keio.ac.jp

Received 22 August 2005; Revised 29 September 2005; Accepted 30 September 2005

**Published online 7 December 2005 in Wiley InterScience (www.interscience.wiley.com). DOI: 10.1002/jnr.20708**

of drugs, and, especially, therapeutic trials, including the transplantation of neural stem cells into the spinal cord. The hSOD1 (G93A) transgenic rats typically present weakness in one hindlimb first. Later, weakness progresses to the other hindlimb and to the forelimbs. Finally, the rats usually become unable to eat or drink, and eventually die. Only subjective and ambiguous analyses were made with regard to the clinical progression of this ALS animal model and objective criteria for evaluating the efficacy of these new treatments have not been determined. For these reasons, we assessed the disease progression quantitatively using five different measures (body weight, inclined plane test, cage activity, SCANET, and righting reflex) and established an easy, noninvasive, and objective evaluation system that is sensitive to small but important abnormalities in the hSOD1 (G93A) transgenic rats. In addition, we created a novel scale, the Motor score, to assess disease progression in the transgenic rats without using special apparatuses. We also examined the validity of these measures as assessment tools for the pathology by investigating the number of spinal motor neurons remaining at the disease stages defined by each measure.

## MATERIALS AND METHODS

### Transgenic Rats

All animal experiments were conducted according to the Guidelines for the Care and Use of Laboratory Animals of Keio University School of Medicine. We used hSOD1 (G93A) transgenic male rats (Nagai et al., 2001) from our colony and their age- and gender-matched wild-type littermates as controls. Rats were housed in a specific pathogen-free animal facility at a room temperature of 23 ± 1°C under a 12-hr light-dark cycle (light on at 08:00). Food (solid feed CE-2, 30kGy; CLEA Japan, Inc.) and water were available ad lib. Transgenic rats were bred and maintained as hemizygotes by mating transgenic males with wild-type females. Transgenic progeny were identified by detecting the exogenous hSOD1 transgene, by amplification of pup tail DNA extracted at 20 days of age by polymerase chain reaction (PCR). The primers and cycling conditions were described previously (Nagai et al., 2001).

### Exploration of Assessment Tools to Measure Disease Progression in the hSOD1 (G93A) Transgenic Rats

We evaluated the usefulness of four different measures to assess disease progression in the transgenic rats. All tests were carried out between 12:00–16:00 and in a double-blind fashion.

**Body weight.** Animals ($n = 9$ for each genotype) were weighed weekly after 30 days of age with an electronic scale. To avoid overlooking the beginning of weight loss, the animals were weighed every second or third day after 90 days of age, the age at which motor neurons are reported to be lost in the lumbar spinal cord (Nagai et al., 2001).

**Inclined plane.** This test was initially established mainly to assess the total strength of the forelimbs and hindlimbs in a model of spinal cord injury (Rivlin and Tator, 1977). Briefly, rats were placed laterally against the long axis of the inclined plane, and the maximum angle at which they could maintain their position on the plane for 5 sec was measured. To assess the strength of both sides of limbs equally, animals were placed on the inclined plane with the right side of the body to the downhill side of the incline, and then with the left side of the body facing downhill. For each rat, the test was carried out three times for each side, and the mean value of the angles obtained for the right side was compared to that obtained for the left. The lower mean value was recorded as the angle for that rat. Animals ($n = 9$ for each genotype) were tested weekly after 70 days of age and every second to third day after 100 days of age.

**Cage activity.** Animals ($n = 8$ for each genotype) were housed individually and monitored every day for all 24 hr (except for the days the cages were changed) after they were 70 days old. Spontaneous locomotor activity in the home cage (345 × 403 × 177 mm) was recorded by an activity-monitoring system (NS-AS01; Neuroscience, Inc., Tokyo, Japan) as described previously (Ohki-Hamazaki et al., 1999). The sensor detects the movement of animals using the released infrared radiation associated with their body temperature. The data were analyzed by the DAS-008 software (Neuroscience, Inc., Tokyo, Japan). To eliminate data variability owing to differences in the baseline movement of each rat, the baseline value was calculated as the mean of movement from 70–90 days of age, during which all rats were considered to move normally. We analyzed the data at each time point as the percentage of the baseline value in defining disease onset with this test.

**SCANET.** For short-term activity, 10 min of spontaneous activity was measured with the automated motion analysis system SCANET MV-10 (Toyo Sangyo Co., Ltd., Toyama, Japan) (Mikami et al., 2002). Animals ($n = 4$ for each genotype) were tested weekly after 30 days of age and every second or third day after 100 days of age. Each rat was individually placed in the SCANET cage for 10 min. Three parameters were measured: small horizontal movements of 12 mm or more (Move 1; M1), large horizontal movements of 60 mm or more (Move 2; M2), and the frequency of vertical movements caused by rearing (RG). To distinguish RG movements from incomplete standing actions, the upper sensor frame was adjusted to 13 cm above the lower sensor frame.

**Righting reflex.** All affected animals were tested for the ability to right themselves within 30 sec of being turned on either side (righting reflex) (Gale et al., 1985). Failure was seen when animals reached the end-stage of disease (Howland et al., 2002), and was regarded as a generalized loss of motor activity. We used this time point, which we call "end-stage," as "death" rather than the actual death of the animal, to exclude the influence of poor food intake and respiratory muscle paralysis on the survival period. All end-stage animals were sacrificed after being deeply anesthetized.

All statistical analyses were carried out with the two-tailed unpaired Student's $t$-test. A $P$-value of $<0.05$ was considered statistically significant.

### Motor Score

To establish our own scoring system for motor function, which could be uniformly applicable to any disease phenotype of this rat model, we examined the common clinical findings

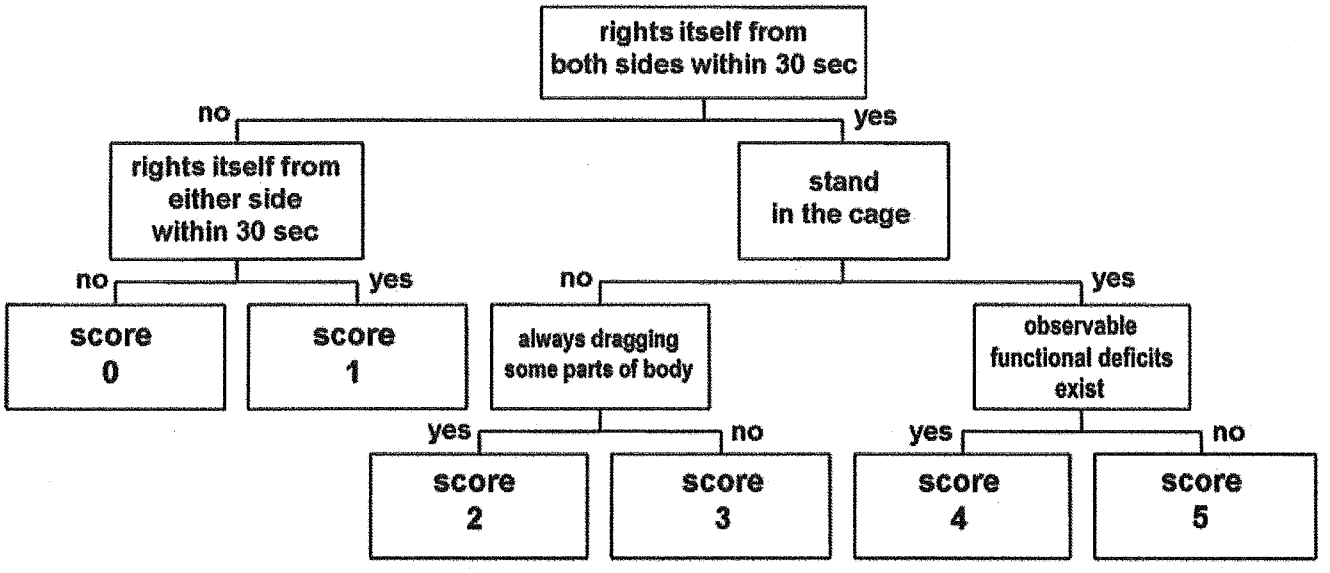


Fig. 1. Chart of Motor score assessment. The degree of motor dysfunction can be assessed by the Motor score as shown in this chart. This scoring system is meant to be used after disease onset, which can be prospectively diagnosed by the inclined plane test (muscle weakness onset). A score of 4 means the same condition as seen for subjective onset (SO). Rats with a score of 5 seem almost as normal as wild-type rats. The detailed testing procedure for the Motor score is described in the text.

of the transgenic rats in detail and assessed their motor functions ($n = 20$). We focused on the following tests: the righting reflex, the ability to stand in the cage, the extent of dragging their bodies when moving, and the existence of observable functional deficits. We evaluated these items sequentially along with the disease progression and classified the rats into six groups by giving them scores between 0 and 5. The scoring chart (Motor score) is shown in Figure 1.

When disease onset in the rats was diagnosed by their scoring $<70°$ on the inclined plane test (muscle weakness onset), the affected rats were tested for righting reflex. If they were unable to right themselves from either side, they were given a score of 0. If they could right themselves from only one side but not the other, they were given a score of 1.

Rats that could right themselves from both sides were examined for the ability to stand in the cage as follows: Rats were observed in the home cage for 1 min to see if they would stand spontaneously (Step 1). When they moved little in the home cage or showed no tendency to stand during Step 1, they were stimulated by being transferred to another cage (Step 2), and then by being returned to their home cage again (Step 3); the transfers were done to activate exploration motivation. During Step 3, the rats were further stimulated by lightly knocking the cage to intensify the motivation to explore. Each step was carried out for 1 min and the test was stopped when the rat stood once. Rats were judged as "unable to stand" if they did not stand, even after all three steps.

Rats that did not stand were subjected to the next test in the open field, where the extent to which they dragged their bodies when moving was assessed. Those who always dragged and could not lift some parts of their bodies except for scrotums and tails at any time were given a score of 2. If they could lift their dragging parts off the ground for even a moment, they were given a score of 3. The phenotype of dragging the forelimbs was different from that of dragging the hindlimbs. As disease progressed, "forelimb-type" rats first began to touch the tips of their noses on the ground, and then began to drag their head and upper trunk as they moved backward with their hindlimbs. "Hindlimb-type" rats dragged their lower trunk and moved forward with their forelimbs.

Finally, rats that had no abnormality in the above-mentioned assessments were examined in detail to see whether they had any observable functional deficits such as paralysis of the limbs or symptoms of general muscle weakness (e.g., walking with a limp, sluggish movement) in the open field. This condition could be judged subjectively and was defined as subjective onset. Rats with any of these symptoms were given a score of 4; otherwise they were given a score of 5.

Because the scores were based on subjective judgment, they might vary depending on the examiner. To examine inter-rater variability, three transgenic rats of different clinical types were examined according to the method described above, recorded on video tape, and subsequently scored by five observers from different backgrounds (Table I). The scores classified by the five observers were statistically analyzed for inter-rater agreement using Cohen's $\kappa$ statistics (Table II). Kappa values can range from 0 (no agreement) to 1.00 (perfect agreement), and can be interpreted as poor ($<0.00$), slight (0.00–0.20), fair (0.21–0.40), moderate (0.41–0.60), substantial (0.61–0.80), and almost perfect (0.81–1.00) (Landis and Koch, 1977). The scores for the three transgenic rats were, on the whole, quite consistent among the five observers, suggesting that the Motor score can be used as an objective method for assessing disease progression.

**TABLE I. Motor Score of Transgenic Rats Assessed by Five Different Observers**

| Transgenic rat | Observer | Days after onset (days) 0 | 1 | 2 | 3 | 4 | 5 | 6 | 7 | 8 |
|---|---|---|---|---|---|---|---|---|---|---|
| #1407 Eventual hindlimb type | | | | | | | | | | |
| | A | 5 | 4 | 4 | | 2 | 2 | 1 | 0 | |
| | B | 4 | 4 | 4 | | 2 | 2 | 1 | 0 | |
| | C | 4 | 4 | 4 | | 2 | 2 | 1 | 0 | |
| | D | 4 | 4 | 4 | | 2 | 2 | 1 | 0 | |
| | E | 4 | 4 | 4 | | 2 | 2 | 1 | 0 | |
| | Mean | 4.2 | 4 | 4 | | 2 | 2 | 1 | 0 | |
| #1470 Pure hindlimb type | | | | | | | | | | |
| | A | 5 | | 4 | 4 | 2 | 2 | 2 | 2 | 0 |
| | B | 5 | | 4 | 3 | 3 | 2 | 2 | 2 | 0 |
| | C | 5 | | 4 | 3 | 2 | 2 | 2 | 2 | 0 |
| | D | 4 | | 4 | 4 | 2 | 2 | 2 | 2 | 0 |
| | E | 4 | | 4 | 3 | 2 | 2 | 2 | 2 | 0 |
| | Mean | 4.6 | | 4 | 3.4 | 2.2 | 2 | 2 | 2 | 0 |
| #1449 Pure forelimb type | | | | | | | | | | |
| | A | 4 | 3 | 3 | 3 | | 2 | 1 | 1 | 0 |
| | B | 4 | 3 | 3 | 3 | | 2 | 1 | 1 | 0 |
| | C | 3 | 3 | 3 | 3 | | 2 | 1 | 1 | 0 |
| | D | 3 | 3 | 3 | 3 | | 2 | 1 | 1 | 0 |
| | E | 4 | 3 | 2 | 2 | | 2 | 1 | 1 | 0 |
| | Mean | 3.6 | 3 | 2.8 | 2.8 | | 2 | 1 | 1 | 0 |

**TABLE II. The kappa Statistics for Inter-Rater Agreement of Motor Score**

| Observers | Transgenic rat (clinical type) #1407 Eventual hindlimb | #1470 Pure hindlimb | #1449 Pure forelimb |
|---|---|---|---|
| A vs. B | 0.82 | 0.69 | 1.00 |
| A vs. C | 0.82 | 0.82 | 0.83 |
| A vs. D | 0.82 | 0.81 | 0.83 |
| A vs. E | 0.82 | 0.70 | 0.69 |
| B vs. C | 1.00 | 0.83 | 0.83 |
| B vs. D | 1.00 | 0.53 | 0.83 |
| B vs. E | 1.00 | 0.66 | 0.69 |
| C vs. D | 1.00 | 0.64 | 1.00 |
| C vs. E | 1.00 | 0.82 | 0.54 |
| D vs. E | 1.00 | 0.81 | 0.54 |

**TABLE III. Clinical Types of hSOD1 (G93A) Transgenic Rats**

| Clinical type | Subtype | *n* | % |
|---|---|---|---|
| Forelimb | Pure | 4 | 8.2 |
| | Eventual | 5 | 10.2 |
| Hindlimb | Pure | 19 | 38.7 |
| | Eventual | 17 | 34.7 |
| General | | 4 | 8.2 |
| Total | | 49 | 100 |

## Real-Time RT-PCR and Western Blot Analysis

Tissue specimens were dissected from the cerebral cortices, cerebella, medullae, and spinal cords (cervical, thoracic, and lumbar spinal cords) of the deeply anesthetized rats, and divided into two portions for total RNA and total protein preparation. Total RNA was isolated and first strand cDNA was synthesized as described previously (Okada et al., 2004). The real time RT-PCR analysis was carried out using Mx3000P (Stratagene, La Jolla, CA) with SYBR Premix Ex Taq (Takara Bio, Inc., Otsu, Japan). The primers used for the analysis were human *SOD1* (5′-TTGGGCAATGTGACTGCTGAC-3′, 5′-AGCTAGCAGGATAACAGATGA-3′), rat *SOD1* (5′-ACTTCGAGCAGAAGGCAAGC-3′, 5′-ACATTGGCCACACCGTCCTTTC-3′), and *β-actin* (5′-CGTGGGCCGCCCTAGGCACCA-3′, 5′-TTGGCCTTAGGGTTCAGAGGGG-3′). The results are presented as ratios of mRNA expression normalized to an inner control gene, *β-actin*. Total protein was prepared in lysis buffer containing 10 mM Tris-HCl (pH 7.6), 50 mM NaCl, 30 mM sodium pyrophosphate, 50 mM sodium fluoride, 20 mM glycerophosphate, 1% Triton X-100, and a protease inhibitor mixture (Complete; Roche Applied Science, Mannheim, Germany). Western blot analysis was carried out by a method established previously. In brief, a 5 μg protein sample of an extract was run on 12% SDS-PAGE, transferred to nitrocellulose, and probed with anti-human SOD1 (1:1,000, mouse IgG, Novocastra Laboratories, Ltd., Benton Lane, UK), and anti-α-tubulin (1:2,000, mouse IgG, Sigma-Aldrich, Inc., Saint Louis, MO). Signals were detected with HRP-conjugated secondary antibodies (Jackson ImmunoResearch Laboratories, Inc., West Grove, PA) using an ECL kit (Amersham Bioscience UK limited, Little Chalfont, UK). Quantitative analysis was carried out with a Scion Image (Scion Corporation, Frederick, MD). The amounts of proteins loaded in each slot were normalized to those of α-tubulin.

## Immunohistochemical Analysis

Rats were deeply anesthetized (ketamine 75 mg/kg, xylazine 10 mg/kg, i.p.) and transcardially perfused with 4% paraformaldehyde/PBS (0.1 M PBS, pH 7.4) for histological examination. Spinal cord tissues were dissected out and post-fixed overnight in the same solution. Each spinal cord was dissected into segments that included the C6, T5, and L3 levels, immersed in 15% sucrose/PBS followed by 30% sucrose/PBS at 4°C, and embedded in Tissue-Tek O.C.T. Compound (Sakura Finetechnical Co., Ltd., Tokyo, Japan). Embedded tissue was immediately frozen with liquid nitrogen and stored at −80°C. Serial transverse sections of each spinal segment were cut on a cryostat at a thickness of 14 μm. The sections were pre-treated with acetone for 5 min, rinsed with PBS three times and permeabilized with TBST (Tris-buffered saline with 1% Tween 20) for 15 min at room temperature. After being blocked in the TNB buffer (Perkin-Elmer Life Sciences, Inc., Boston, MA) for 1 hr at room temperature, the sections were incubated at 4°C overnight with an anti-choline acetyltransferase (ChAT) polyclonal antibody (AB144P, Goat IgG, 1:50; Chemicon International, Inc., Temecula, CA). After being washed with PBS three times, the sections were incubated for 2 hr at room temperature with a biotinylated secondary antibody (Jackson ImmunoResearch Laboratories, Inc.). Finally, the labeling was developed using the avidin-biotin-peroxidase complex procedure (Vectastain ABC kits; Vector Laboratories, Inc., Burlingame, CA) with 3,3-diaminobenzidine (DAB; Wako Pure Chemical Industries, Ltd., Osaka, Japan) as the chro-

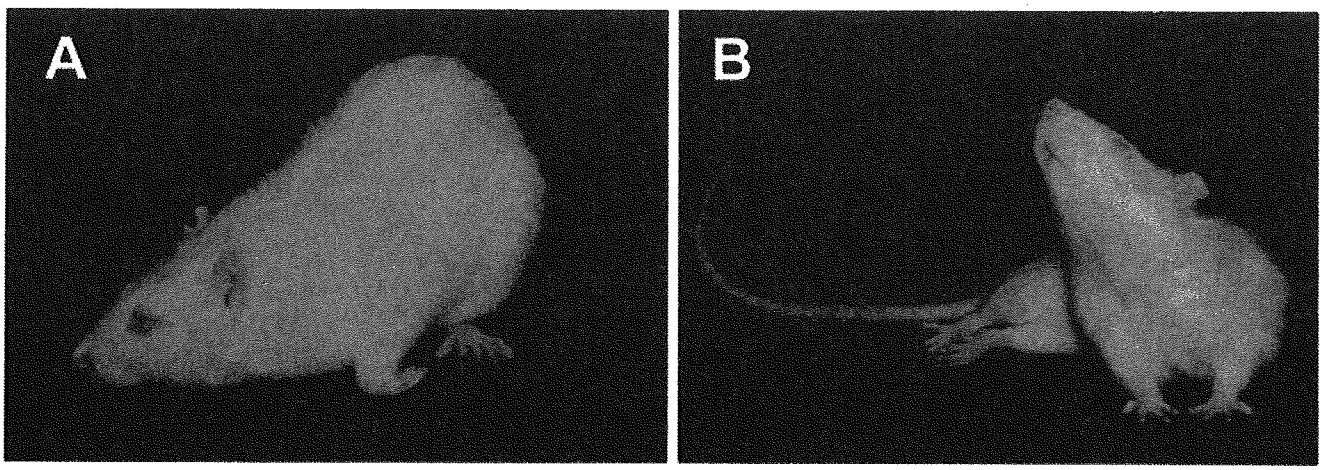


Fig. 2. Characteristic appearance of hSOD1 (G93A) transgenic rats. **A:** Forelimb type. The rat was unable to raise its head and was obligated to take a posture of raising the lumbar region, as indicated, because of the paralyzed forelimbs. **B:** Hindlimb type. The rat showed paraplegia, but was able to raise its head and upper trunk with its non-paralyzed forelimbs.

mogen. Immunohistochemical images were examined with a Zeiss-AxioCam microscope system.

Motor neurons bearing ChAT-immunoreactivity in laminae VII, VIII, and IX of the ventral horn were counted in every tenth section (5 sections total for each segment) for each of the C6, T5, and L3 segments. Only the neurons that showed labeling above background level and were larger than 20 μm in diameter were counted. The numbers of motor neurons in all segments (C6, T5, and L3) were summed for each animal to evaluate not only the local motor neuron loss, but the generalized loss of motor neurons throughout the spinal cord of each animal ($n = 3$ for each genotype at each time point). We next examined the correlation between the number of residual motor neurons and the results of the functional analyses described in this study. Statistical analysis was carried out with two-tailed unpaired Student's *t*-test. A *P*-value of $<0.05$ was considered statistically significant.

## RESULTS

### Clinical Types of hSOD1 (G93A) Transgenic Rats

Because we noticed variations in the disease phenotypes expressed by the G93A rats, we classified 49 rats into three clinical categories according to the location of initial paralysis. The clinical types were: the forelimb type, hindlimb type, and general type (Table III). Rats whose paralysis started in the forelimbs and progressed to the hindlimbs were defined as the "forelimb type." In contrast, rats whose paralysis started from the hindlimbs and progressed to the forelimbs were defined as the "hindlimb type." A typical appearance for the forelimb and hindlimb types is shown in Figure 2. Other rats, which showed simultaneous paralysis in the forelimbs and hindlimbs, were categorized as the "general type".

In addition, we classified the forelimb- and hindlimb-type rats into two subtypes, the pure and eventual types, based on the timing of the initial paralysis (Table III). Rats of the pure type showed paralysis that was limited to one or more of the four limbs as the initial observable deficit. Those of the eventual type initially showed symptoms of general muscle weakness (e.g., walking with a limp, sluggish movement), but without unequivocal limb paralysis. In the eventual type animals, paralysis of one of the limbs became apparent later. The ratio of each subtype is shown in Table III.

### Evaluation of Disease Progression in the hSOD1 (G93A) Transgenic Rats

Although the transgenic rats varied in their clinical types, all four measures of disease progression (body weight, inclined plane test, cage activity, and SCANET) showed significant differences between the transgenic and wild-type rats (Fig. 3).

In contrast to the continuous weight gain in wild-type rats, the body weight in the affected rats ceased to increase and gradually decreased, with peak body weight attained around 110–120 days of age ($P < 0.05$, after 112 days of age) (Fig. 3A).

In the inclined plane test, initially both the transgenic and wild-type rats uniformly scored 75–80 degrees, after several training trials. However, the transgenic rats showed a significant decline in performance compared to their wild-type littermates from 120 days of age (Fig. 3B).

In the cage activity measurement, the movements of the wild-type rats remained stable, whereas those of the transgenic rats declined rapidly after 125 days of age (Fig. 3C).

In the SCANET test, even the wild-type rats showed decreased movements for all parameters (M1, M2, RG) in the late observation period, though they showed no abnormality in their motor functions. This might be because they had acclimated to the SCANET cage. The movement score of the transgenic rats was consistently worse than that of the wild-type rats after

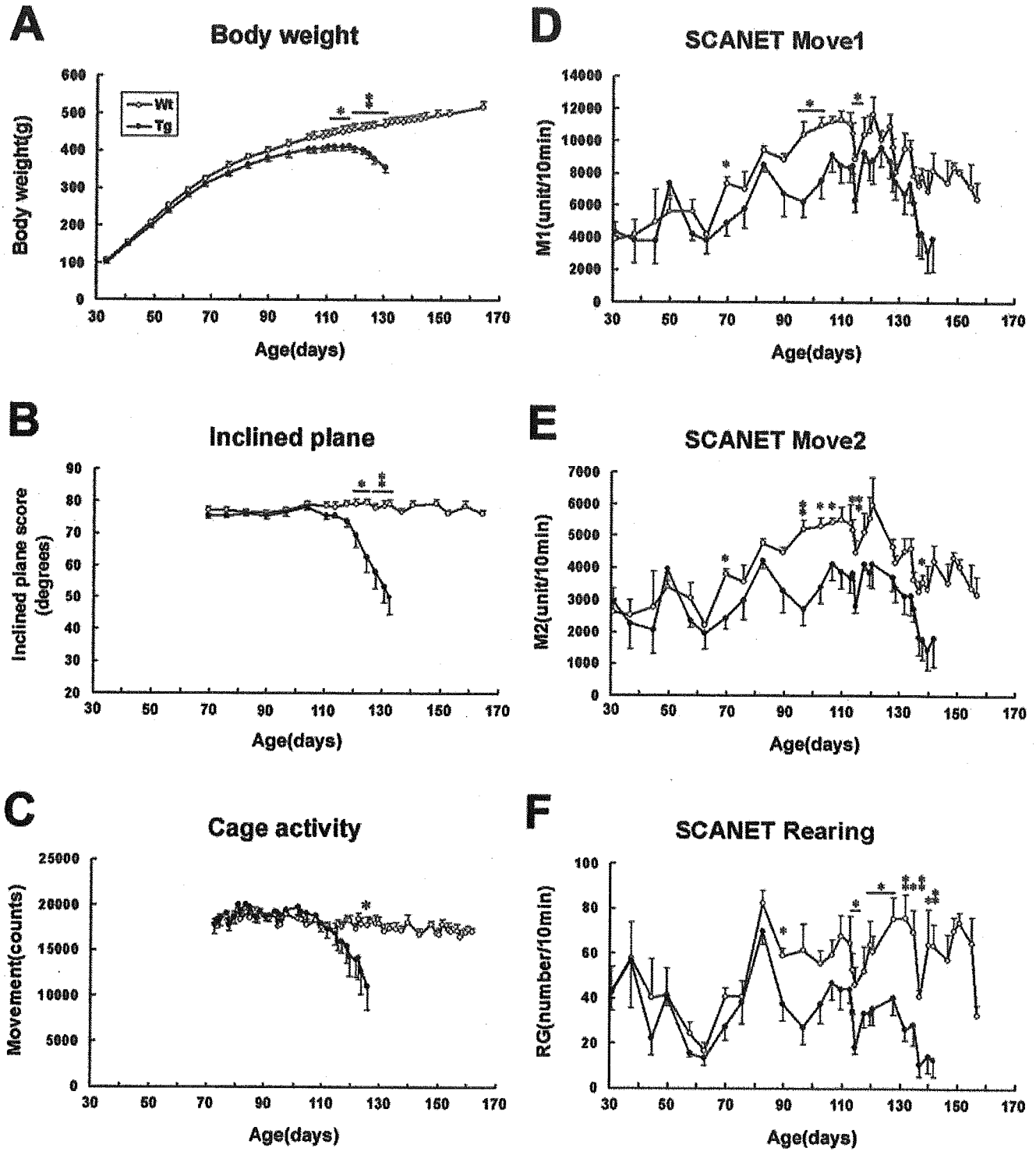


Fig. 3. Disease progression in hSOD1 (G93A) transgenic rats monitored by four effective measures. **A:** Body weight. The weight gain of the transgenic group stopped at around 110–120 days. The difference became statistically significant at 112 days of age ($n = 9$ for each genotype). **B:** Inclined plane. The wild-type group scored 75–80° throughout the period, whereas the score of the transgenic group declined. The difference became statistically significant at 120 days of age ($n = 9$ for each genotype). **C:** Cage activity. The movements of the wild-type group were stable, whereas the scores of the transgenic group declined. Significance was reached at 125 days of age ($n = 8$ for each genotype). **D–F:** SCANET. For all parameters (M1, M2, RG), the movement scores of the transgenic group became constantly worse than those of the wild-type group after 60 days of age. The differences between the groups increased markedly after 90 days of age. Significance was attained beginning at 67 days of age for M1 and M2, and at 87 days of age for RG ($n = 4$ for each genotype). The comparison between the wild-type and transgenic groups was stopped when the first of the transgenic rats reached the end-stage of the disease and was sacrificed. Mean ± SEM. $*P < 0.05$. $**P < 0.01$; two-tailed unpaired Student's *t*-test.

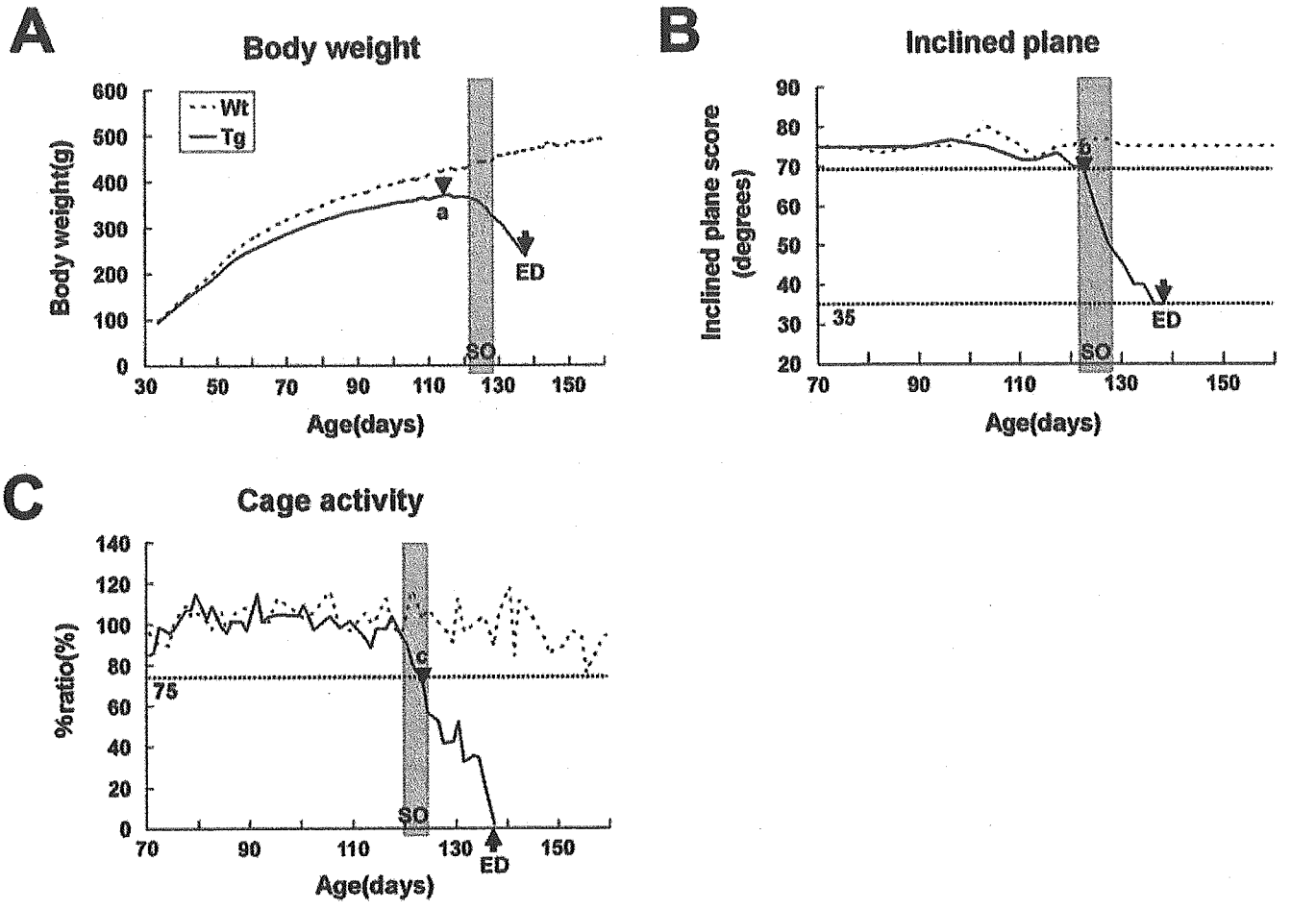


Fig. 4. Schematic presentation of the results from the body weight (**A**), inclined plane test (**B**), and cage activity (**C**) assessments. The onset defined by each measure (black arrowheads) and the end-stage of the disease (ED, black arrows) are indicated in the figures. a, pre-symptomatic onset: the day the transgenic rats scored their maximum body weight. b, muscle weakness onset: the earliest day the transgenic rats scored <70° in the inclined plane test. c, hypo-activity onset: the earliest day the transgenic rats scored <75% of the mean movements from 70–90 days of age in the cage activity measure. SO, subjective onset: the earliest day that observable functional deficits such as paralysis of the limbs or symptoms of general muscle weakness were observed subjectively in the open field (the gray shaded region in A–C).

60 days of age for all parameters (M1, M2, RG), however, even after the wild-type animals showed the decrease in their movement scores. The differences between the two groups increased markedly after 90 days of age for M1, M2, and RG (Fig. 3D–F). The performance of each rat fluctuated so markedly that the SCANET test seems to be inappropriate for statistical analysis.

### Onset, End-Stage, and Duration of Disease in hSOD1 (G93A) Transgenic Rats

Using the quantitative analysis of disease progression by body-weight measurement, the inclined plane test, and cage activity, as described above, we defined three time points of "objective onset," as shown in Figure 4. The SCANET results did not allow us to define a time of objective onset, because we could not establish a stable baseline level using the data from the highly variable measurements we obtained, even for wild-type rats. The righting reflex failure was useful for detecting the time point of end-stage disease, which we defined as the generalized loss of motor activity in affected rats. A total of 20 transgenic rats assessed by body weight and the inclined plane test were analyzed for the day of objective onset, end-stage, and duration of the disease. The cage activity data from the eight transgenic rats were obtained simultaneously. The results are shown in Table IV.

The day the transgenic rats reached their maximum body weight was defined as pre-symptomatic onset (113.6 ± 4.8 days of age, black arrowhead in Fig. 4A, Table IV). This onset was judged retrospectively and always preceded the subjective onset (gray shaded region, Fig. 4A), which was determined by observable functional deficits in the open field, such as paralysis of limbs and symptoms of general muscle weakness. The

**TABLE IV. Onset, End-Stage, and Duration in Days of Disease in hSOD1 (G93A) Transgenic Rats**

| Evaluation methods | Body weight and inclined plane ($n$ = 20) | Cage activity ($n$ = 8) |
|---|---|---|
| Objective onset | | |
| Pre-symptomatic onset[a] | 113.6 ± 4.8 (103–124) | |
| Muscle weakness onset[b] | 125.2 ± 7.4 (110–144) | |
| Hypo-activity onset[c] | | 122.8 ± 9.2 (109–139)[c] |
| Subjective onset (SO)[d] | 126.5 ± 7.1 (113–147) | 121.3 ± 9.8 (109–140) |
| End-stage disease (ED)[e] | 137.8 ± 7.1 (128–155) | 134.1 ± 8.2 (122–149) |
| Duration[f] | | |
| ED-a[g] | 24.3 ± 6.5 | |
| ED-b[h] | 12.6 ± 3.5 | |
| ED-c[i] | | 11.4 ± 1.3 |

Values are means ± SD.
[a] Maximum of body weight.
[b] Less than 70 degrees in the inclined plane test.
[c] Less than 75% in the mean movements of 70-90 days in the cage activity.
[d] Observable functional deficits.
[e] Righting reflex failure.
[f] Difference in days between ED and each onset;
[g] between ED and pre-symptomatic onset,
[h] between ED and muscle weakness onset,
[i] between ED and hypo-activity onset.

**TABLE V. Comparison of the Onset, End-stage, and Duration in Days of Disease in the Forelimb-type and the Hindlimb-type Rats**

| | Forelimb type ($n$ = 4) | Hindlimb type ($n$ = 14) | General type* ($n$ = 2) |
|---|---|---|---|
| Pre-symptomatic onset[a] | 112.5 ± 6.7 | 114.6 ± 4.3 | (108.5) |
| Muscle weakness onset[b] | 125.8 ± 2.8 | 126.7 ± 7.3 | (113.5) |
| End-stage disease (ED)[c] | 134.0 ± 2.4 | 140.1 ± 7.1 | (129.5) |
| Duration[d] | | | |
| ED-a[e] | 21.5 ± 8.5 | 25.5 ± 6.2 | (21) |
| ED-b[f] | 8.3 ± 1.0 | 13.4 ± 3.0 | (16) |

Values are mean ± SD.
* Values of general-type rats are listed in parenthesis for reference.
[a] Maximum of body weight.
[b] Less than 70 degrees in the inclined plane test.
[c] Righting reflex failure.
[d] Difference in days between ED and each onset;
[e] between ED and pre-symptomatic onset,
[f] between ED and muscle weakness onset.

pre-symptomatic onset was the most sensitive of all the onset measures described in this study (Table IV).

The first day the transgenic rats scored <70° in the inclined plane test was defined as the muscle weakness onset (black arrowhead, Fig. 4B). We could judge this onset prospectively. Muscle weakness onset (125.2 ± 7.4 days of age, Table IV) was usually recorded before or at almost the same time as the subjective onset (8 days before to 1 day after, gray shaded region, Fig. 4B and 126.5 ± 7.1 days of age, Table IV). The day the transgenic rats scored 35° or less on the inclined plane test coincided with the day of righting reflex failure (black arrow, Fig. 4B).

The first day the transgenic rats scored <75% of their baseline movements in the cage activity test was defined as hypo-activity onset (black arrowhead, Fig. 4C and 122.8 ± 9.2 days of age, Table IV). We could also judge this onset prospectively. Hypo-activity onset was recorded 1 day before to 4 days after the subjective onset (SO, shown as the gray shaded region in Fig. 4C and 121.3 ± 9.8 days of age, Table IV). A 0% movement score for cage activity was seen at almost the same time as righting reflex failure (black arrow, Fig. 4C). Although disease onset and end-stage could be objectively defined with these methods, they had a wide range, of about 1 month, because of the diversity of the phenotypes (Table IV).

## Differences in Disease Courses Between the Forelimb- and Hindlimb-Type Rats

Because we noticed variability in disease courses among different clinical types of hSOD1 (G93A) rats, we next assessed disease progression in 20 transgenic rats with forelimb- ($n$ = 4), hindlimb- ($n$ = 14), and general- ($n$ = 2) type, using the probability of objective

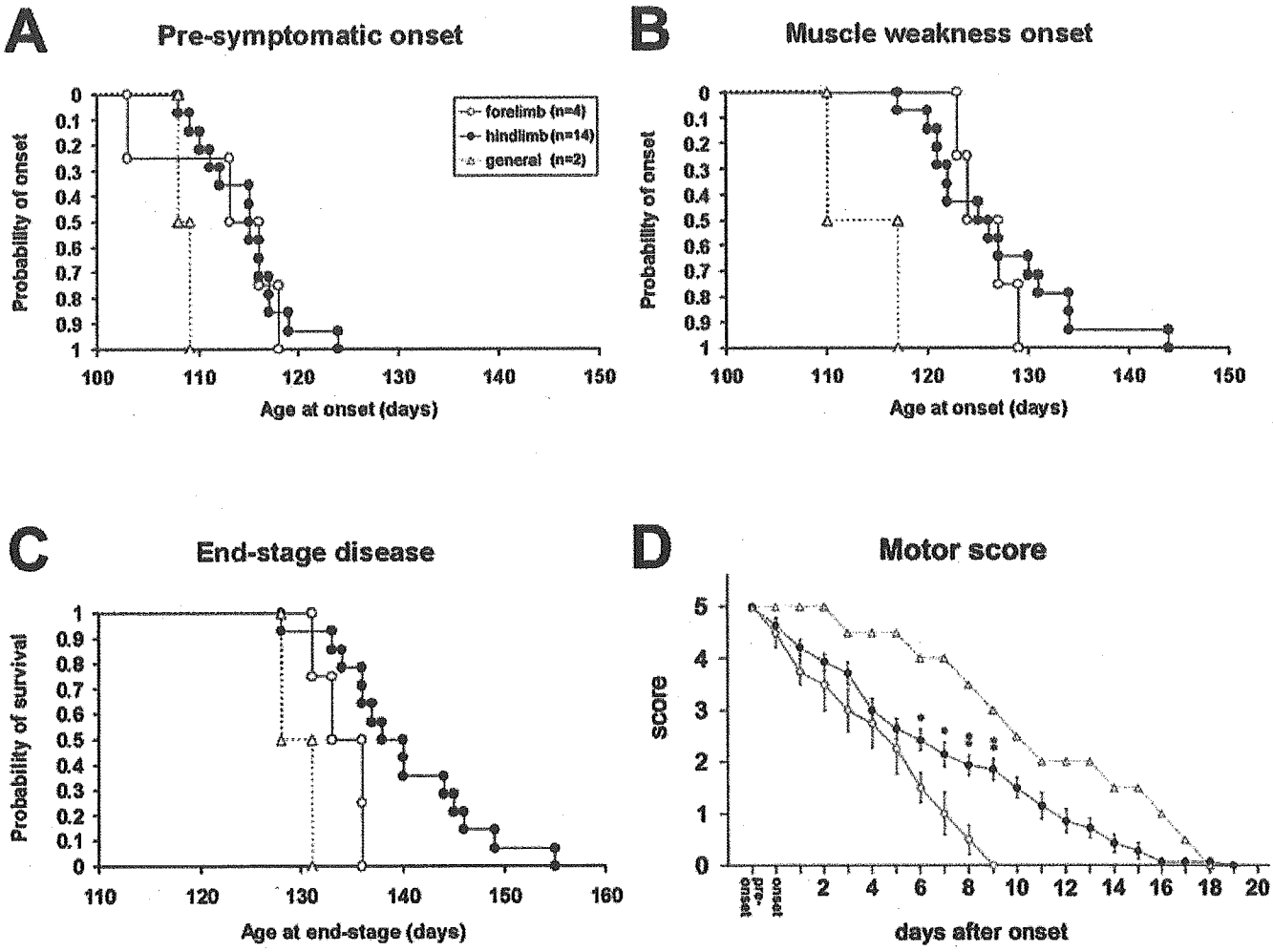


Fig. 5. Comparison of onset, end-stage, and disease progression in the forelimb-type ($n = 4$), and the hindlimb-type ($n = 14$) rats. Data from the general-type rats are also shown as dotted lines. **A,B:** The probability of the objective onsets. We did not see any differences in the probability of the objective onsets defined by body weight measurement (pre-symptomatic onset) and the inclined plane test (muscle weakness onset) between the forelimb- and hindlimb-type rats. **C:** The probability of survival as defined by end-stage disease. Survival was significantly shorter in the forelimb-type than in the hindlimb-type rats ($P < 0.05$, Log-rank test). **D:** Assessment of disease progression using the Motor score. Affected rats were evaluated after muscle weakness onset. The forelimb type worsened more quickly than the hindlimb type. Score decline correlated well with the exacerbation of symptoms in both clinical types, clearly and objectively. Bars = means ± SEM. Statistically significant differences between forelimb and hindlimb types are indicated in the figures. $*P < 0.05$. $**P < 0.01$; two-tailed unpaired Student's $t$-test.

onsets (pre-symptomatic onset and muscle weakness onset), the probability of survival defined by end-stage disease (failure in righting reflex), and the Motor score (Table V, Fig. 5). We did not see any differences in the objective onsets between the forelimb- and hindlimb-type rats (Fig. 5AB, Table V). However, survival as defined by end-stage disease was significantly shorter in the forelimb-type than in the hindlimb-type rats ($P < 0.05$, Log-rank test, Fig. 5C). Moreover, the duration of the disease calculated from the muscle weakness onset was also significantly shorter in the forelimb-type (8.3 ± 1.0 days) than in the hindlimb-type rats (13.4 ± 3.0 days) (see ED − b, $P < 0.01$, two-tailed unpaired Student's $t$-test, Table V).

The courses of functional deterioration evaluated by the Motor score after onset (muscle weakness onset) for each clinical type were well represented by the declines in their scores (Fig. 5D). The assessment by the Motor score also showed that disease progression in the forelimb type was more rapid than that in the hindlimb type (Fig. 5D).

Our results raise the question of why this variability in the disease course of each clinical type was observed. We speculated that there might be correlation between clinical type in G93A rats and the amount of locally expressed mutant hSOD1 (G93A) gene product. Therefore, we next investigated expression of the mutant hSOD1 gene in each segment of the spinal cord (cervical, thoracic, and lumbar) in the forelimb- and

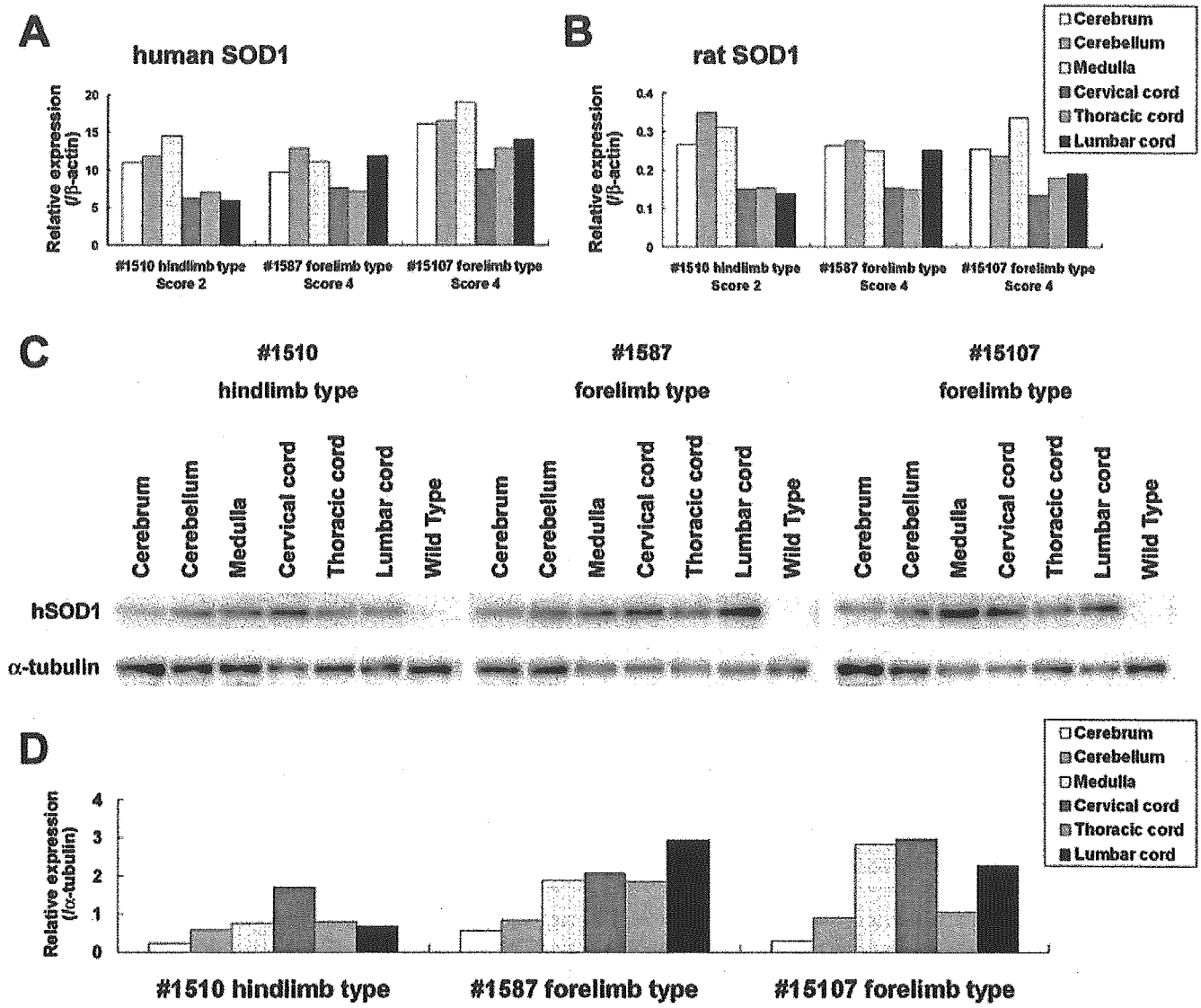


Fig. 6. The expression of mutant hSOD1 mRNA and protein in the cerebral cortex, cerebellum, medulla, and spinal cord (cervical, thoracic, and lumbar) of forelimb- and hindlimb-type rats. **A,B:** The amounts of human (A) and endogenous rat (B) SOD1 mRNA normalized to those of *β-actin* were quantified by real time RT-PCR analysis. **C,D:** Western blot analysis of the mutant hSOD1 protein was carried out in the same rats. Quantitative analysis was carried out with a Scion Image. The amounts of proteins were normalized to those of α-tubulin (D).

hindlimb-type rats by real time RT-PCR and Western blot analysis. However, at least at the stages after the apparent onset of muscle weakness, neither forelimb-type (#1587, Score 4 and #15107, Score 4) nor hindlimb-type rats (#1510, Score 2) necessarily expressed larger amounts of the mutant hSOD1 (G93A) transgene in the cervical cord or in the lumbar cord, respectively, at the mRNA and the protein level (Fig. 6). We also investigated the expression of endogenous rat SOD1 mRNA in the same rats by REAL TIME RT-PCR (Fig. 6B). Distribution of endogenous rat SOD1 mRNA expressed in each segment of the spinal cord showed almost the same pattern as that of mutant hSOD1 mRNA. The expression of endogenous rat SOD1 mRNA was lower than that of mutant hSOD1 mRNA. Thus, we could not detect any definite correlation between the hSOD1 (G93A) transgene local expression profile in the spinal cord and the phenotypes of G93A rats for either the forelimb-type or the hindlimb-type rats (Fig. 6).

## Reduction in the Number of Spinal Cord Motor Neurons at Different Disease Stages

We examined histo-pathological changes in the spinal cords of the transgenic rats in comparison with those